SMHI

COMPARISON OF AREAL PRECIPITATION ESTIMATES AND THEIR PERFORMANCE IN RUNOFF MODELLING: A CASE STUDY FOR A CENTRAL SWEDISH CATCHMENT

Jonas Olsson, Barbro Johansson, Gun Grahn, Sofia Fogelberg
Swedish Meteorological and Hydrological Institute, SE-601 76 Norrköping, Sweden

1 INTRODUCTION

The present report was prepared within Work package 9, *Assessment of the bias, spatial patterns and temporal variability of errors in the different sources of areal precipitation estimates*, of CARPE DIEM (*Critical Assessment of available Radar Precipitation Estimation techniques and Development of Innovative approaches for Environmental Management*). Contract Nº EVG1-CT-2001-0045.

The overall aim within CARPE DIEM is to develop improved techniques for flood forecasting. This requires an improved understanding and observation of preceding atmospheric conditions, that develop into severe rainfall (and, in turn, flooding) events. Crucial for accurate flood forecasting is an accurate estimate of areal precipitation, its magnitude and distribution over a catchment. Such estimates can be obtained from a wide range of sources, including rain gauges, weather radars and NWP models. Each source has its own characteristics and advantages, but also error and bias levels. Often flood forecasting is based mainly on one of the sources. However, with today's widespread production and high level of access to (real-time) data from the various sources, the possibility to improve forecasting by utilising data from several sources is apparent.

In order to evaluate the accuracy of the data from each source, and assess the benefits from their combined use, their characteristics need to be compared. In the present study, areal precipitation estimates from five sources - NWP model, weather radar, rain gauges and two versions of a mesoscale analysis - over a specific catchment during a specific time period are compared in two stages. In the first stage, spatial and temporal properties of the precipitation estimates are compared. In the second stage, the precipitation estimates are used to drive the HBV hydrological model, in order to investigate the effect of the estimates' errors and biases on both runoff simulation and forecasting.

The data are described in Section 2 and the comparative analyses in Section 3. Results in terms of precipitation are shown in Section 4 and in terms of runoff in Section 5. Finally, some conclusions are drawn in Section 6.

2 DATA SOURCES AND ANALYSES

The area studied is the Gimån catchment in central Sweden, centred at approximately 62.8ºN and 15.5ºE (Figure 1). The catchment area is 4 300 km² with a mean altitude of 340 m.a.s.l. (range: 20-540 m.a.s.l.) and a mean annual precipitation of ~700 mm. An area of 72×120 km (8 640 km²), covering the Gimån catchment was selected as the study region and used when extracting data from the different sources described below (Section 2.1-2.4). Later in CARPE DIEM, the accuracy of runoff estimates from different sources of areal precipitation will be evaluated in the Gimån catchment by applying the hydrological HBV model (Lindström et al., 1997).

For the present comparison, data from year 2002 were used. Although a longer time period would have been preferable, 2002 was selected as for this year consistent data from all sources below were readily available. Generally, 2002 was a slightly dry year in the region, with a total precipitation of ~90% the long-term average. In particular late summer and autumn were drier than a normal year. Mean temperature in the region in 2002 was ~1.5°C higher than the long-term average (SMHI, 2002).

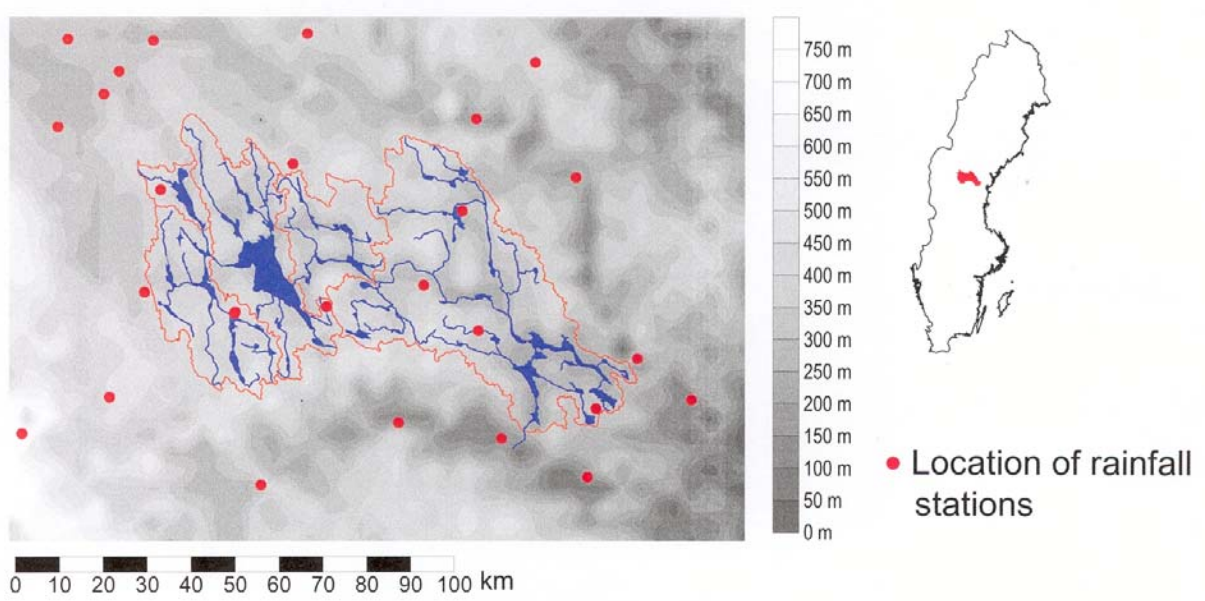

Figure 1. Location and characteristics of the Gimån catchment.

2.1 NWP model (HIRLAM)

The numerical weather prediction model HIRLAM (High Resolution Limited Area Model) has been jointly developed by the weather services in Sweden, Norway, Finland, Denmark, Iceland, Ireland, the Netherlands and Spain. The HIRLAM based precipitation estimates are dependent on the model characteristics, especially the physics parameterisations. The model integration area of the SMHI HIRLAM version used in this study consists of 162×142 horizontal grid points at 22×22 km resolution and 31 vertical levels. Semi-Lagrangean time integration and a fourth order implicit horizontal diffusion scheme are used. The physics package included a first order local vertical diffusion scheme (Louis, 1979), a cloud and condensation scheme based on explicit forecasts of cloud water (Sundqvist et al., 1989) and a radiation scheme based on Savijärvi (1989).

For the details of the various components of the HIRLAM forecasting system we refer to Undén et al. (2002) and Källén et al. (1996).

2.2 Radar (RADAR)

The accumulated precipitation radar product is based on reflectivity products and synoptical observations. Gauge adjustment is achieved by the method of Koistinen and Puhakka (1981) with a number of modifications (Michelson et al., 2000). Gauge accumulations are corrected using an implementation of the Dynamic Correction Model presented by Førland et al. (1996), before they are used for the gauge adjustment (Michelson, 2003). If G denotes gauge observation and R the simultaneous radar observation, a general relationship between log(G/R) and range from the radar is derived using radar and gauge pairs from a 7-day moving time window. Depending on the number and quality of available synoptical observations, this relationship can either be based on a parabolic regression or just the average log(G/R) value. The result is a field in which the quantitative accuracy is largely determined by the gauge values and in which the spatial distribution is determined by the radar data. The horizontal resolution of the radar products is 2×2 km, transformed from polar co-ordinates, and the temporal resolution is 3 h.

Further information can be found in Michelson et al. (2000) and Koistinen and Michelson (2002).

2.3 Gauges (PTHBV)

PTHBV is a gridded precipitation data base, intended to use as input in the HBV hydrological model. The grid is created by optimal interpolation from all available precipitation stations, corrected for

observation losses. In the interpolation scheme, frequencies of wind direction and wind speed are included in the description of the topographic influence.

The horizontal resolution of the PTHBV grid is 4×4 km and precipitation is available as 24-h accumulations.

Further information about the interpolation procedure can be found in Johansson (2002).

2.4 Mesoscale analysis (MA22 and MA11)

In the mesoscale analysis system at SMHI, MESAN, manual observations, automatic station data, satellite and radar imagery are combined by optimal interpolation. Representativity and quality of each observation is taken into account in the interpolation, and the information content dependency on distance is modelled by so-called structure functions. Precipitation analysis is performed using a variable first guess, which makes it possible to increase spatial resolution in data-sparse areas. The description of the error varies as a function of the prevailing weather situation (or precipitation amount). Generally, it is based on a statistically established relation between wind, orography and variations in friction and latitude, and approximately 50% of the observed climatological variance can be explained.

MESAN is run in two versions, a real-time analysis in a 22×22 km grid (MA22) and a climate-corrected analysis in a 11×11 km grid (MA11). From the real-time analysis, in which HIRLAM output (Section 2.1) is used as the first guess in the optimal interpolation procedure, 12-h precipitation accumulations based on synoptical observations were used. From the climate-corrected analysis, 24-h accumulations based on synoptical observations and corrected data from climate stations were used, and in this case the first guess consists of 12-h real-time analyses.

Further information can be found in Häggmark et al. (1997, 2000).

2.5 Data preparations

Data from all sources were converted to the same temporal and areal resolution.

The highest common temporal resolution was 24 h. To achieve this for the HIRLAM output, for each day the +6h forecasted accumulated precipitation was subtracted from the +30h forecast. For RADAR eight 3-h composites were summed and for MA22 two 12-h accumulations were summed, to generate 24-h accumulations.

The highest common areal resolution was 22×22 km. In order to compare spatial variability, all sources of a higher resolution (RADAR, PTHBV, MA11) were averaged to a comparable resolution. (The nodes in the resulting averaged grid did not, however, coincide with the nodes of HIRLAM and MA22; see Appendix 2.) A 22×22 km resolution implies 20 grid nodes in the study area.

For each day and source, a mean areal precipitation was calculated.

3 COMPARATIVE ANALYSES

3.1 Precipitation

Temporal analyses comprised calculations of descriptive statistics (sum, standard deviation, maximum value, percentage of dry days (defined as a mean areal precipitation less than 0.1 mm)) of the daily areal mean values, both for the total series and for individual months. Autocorrelation (lag 1-14 days) was computed for the total series.

Areal analyses comprised calculations of areal standard deviation, both for the 2002 total precipitation in each grid node, and for each day (with a mean areal precipitation greater than 0.1 mm). From the daily standard deviations, mean values were calculated both for the total series and for individual

months. Further, areal correlation as a function of distance was computed for the total series. For the distance, 10-km bins were used (between 25 and 115 km) in which correlations were averaged.

3.2 Runoff

3.2.1 The HBV model

The HBV model (Bergström, 1976, 1992; Lindström et al., 1997) is a rainfall-runoff model which includes conceptual numerical descriptions of hydrological processes at the catchment scale. In different model versions HBV has been applied in more than 40 countries all over the world. It has been applied to countries with such different climatic conditions as for example Sweden, Zimbabwe, India and Colombia. The model has been applied for scales ranging from lysimeter plots (Lindström and Rodhe, 1992) to the entire Baltic Sea drainage basin (Bergström and Carlsson, 1994; Graham, 1999). The model is used for flood forecasting in the Nordic countries, and many other purposes, such as spillway design floods simulation (Bergström et al., 1992), water resources evaluation (for example Jutman, 1992, Brandt et al., 1994), nutrient load estimates (Arheimer, 1998).

The general water balance in the HBV model can be described as

$$P - E - Q = \frac{d}{dt}\left[SP + SM + UZ + LZ + lakes\right] \qquad (1)$$

where P is precipitation, E is evapotranspiration, Q is runoff, SP is snow pack, SM is soil moisture, UZ is upper groundwater zone, LZ is lower groundwater zone, and *lakes* is the lake volume. Input data are observations of precipitation, air temperature and estimates of potential evapotranspiration. The time step is usually one day, but it is possible to use shorter time steps. The evaporation values used are normally monthly averages although it is possible to use daily values. Air temperature data are used for calculations of snow accumulation and melt. It can also be used to adjust potential evaporation when the temperature deviates from normal values, or to calculate potential evaporation. If none of these last options are used, temperature can be omitted in snowfree areas.

The model consists of subroutines for meteorological interpolation, snow accumulation and melt, evapotranspiration estimation, a soil moisture accounting procedure, routines for runoff generation and finally, a simple routing procedure between subbasins and in lakes. It is possible to run the model separately for several subbasins and then add the contributions from all subbasins. Calibration as well as forecasts can be made for each subbasin. For basins of considerable elevation range a subdivision into elevation zones can also be made. This subdivision is made for the snow and soil moisture routines only. Each elevation zone can further be divided into different vegetation zones (e.g., forested and non-forested areas).

Applying the model necessitates calibration of a number of free parameters (around 10 in the present application). The model is equipped with an automatic calibration routine (e.g., Lindström, 1997). The standard calibration criterion RV is a compromise between the traditional efficiency measure R^2 (Nash and Sutcliffe, 1970) and the relative volume error RD combined as

$$RV = R^2 - w \cdot \left|RD\right| \qquad (2)$$

where w is a weight typically close to 0.1. The optimisation is made for one parameter at a time, while keeping the others constant. The one-dimensional search is based on a modification of the Brent parabolic interpolation (Press et al., 1992).

3.2.2 HBV set-up, calibration and execution

The HBV model has been set up for the Gimån catchment (Figure 1). As indicated in the figure, the catchment was divided into five subbasins, each specified in terms of altitude, vegetation and lake zones.

Model calibration was performed by the automatic calibration routine described above (Section 3.2.1) using 20 years of precipitation and temperature data (1982-2001) from the PTHBV data base (Section 2.3). In the catchment, two discharge stations were available; one in the outlet of the four smaller subbasins in the western part of the catchment, and one in the outlet of the entire catchment in the south-eastern corner (Figure 1). Therefore calibration was performed in two steps. In the first step parameter values were obtained for the four western subbasins by calibration on the local outlet (station name: Gimdalsbyn), and the second step parameters for the eastern subbasin were fixed by calibration on the total catchment outlet (station name: Torpshammar). The result of the calibration is shown in Figure 2. For Gimdalsbyn, the R^2 for the calibration period is 0.8965 and the relative volume error 0.00004; for Torpshammar the values are 0.903 and 0.0016, respectively.

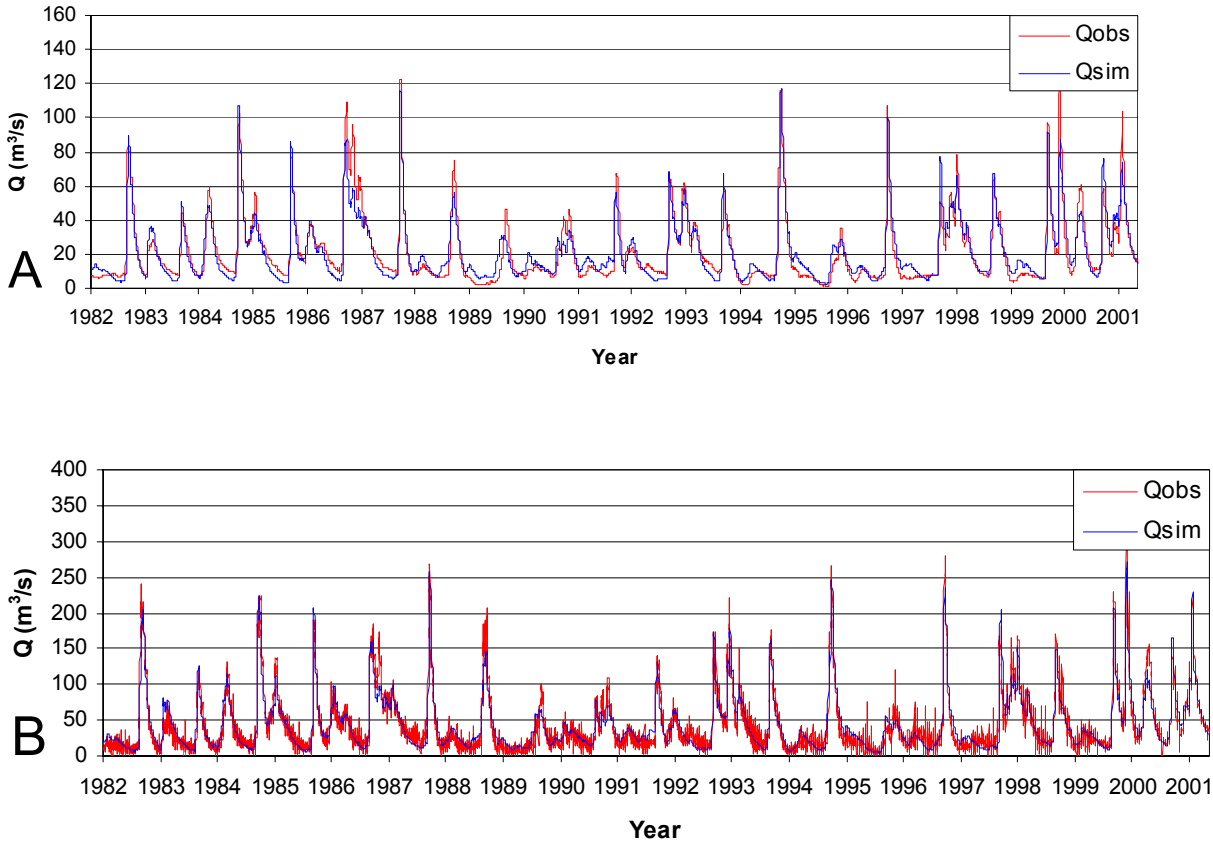

Figure 2. Time series of observed and simulated discharge during the calibration period (1982-2001) for Gimdalsbyn (a) and Torpshammar (b).

Gridded precipitation data from the different sources were transformed into HBV input format, i.e., daily mean precipitation in each subbasin. For each subbasin, this was achieved by identifying all the overlapping grid cells, estimating the fraction of each grid cell located within the subbasin, and calculating an area-weighted subbasin mean precipitation from the grid values.

The calibrated HBV model was run for year 2002 using the different types of precipitation input, and compared with the observed discharge in stations Gimdalsbyn and Torpshammar (Figure 3). Concerning station Gimdalsbyn, the observed runoff exhibits a decreasing trend from January (~15 m^3/s) until early April (<10 m^3/s) , when spring flood starts. The spring flood reaches its peak in early May (~50 m^3/s), after which a rapid recession takes place until late June (~15 m^3/s). A comparison with Figure 2a shows that the spring flood peak is rather low, below average. The second half of the year is characterised by a decreasing discharge which reaches its minimum in mid-October (<2 m^3/s), to finally increase slowly to ~4 m^3/s at the end of the year. Concerning station Torpshammar, the more irregular behaviour of the observed runoff, as compared with Gimdalsbyn, is due to that this inflow

has not been measured directly but estimated from measured values of lake outflow and change in lake volume. The latter is based on water level observations which are inherently uncertain because of natural fluctuations, and a small difference in water level may have a great impact on lake volume and in turn estimated discharge. The annual pattern is naturally similar to Gimdalsbyn, but the spring flood is notably more pronounced and also a summer peak is more clear than for Gimdalsbyn. The spring flood peak runoff in Torpshammar, ~175 m³/s, is slightly above average (Figure 2b).

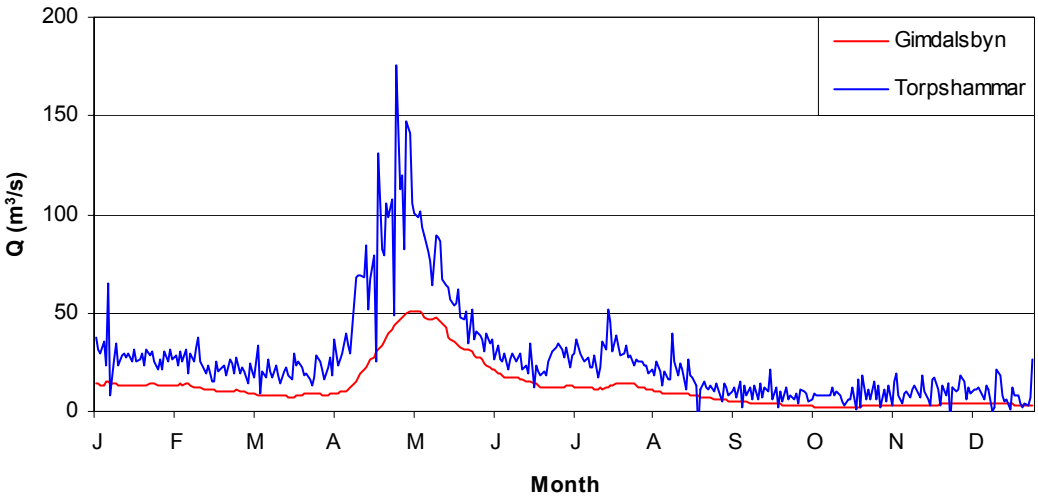

Figure 3. Time series of observed discharge during 2002 for Gimdalsbyn and Torpshammar.

As initial model state at the start of the simulations on 020101, the final state from the calibration period (1982-2001) was used for all sources. To study the effect of only precipitation input, in the runoff simulations the same temperature input was used for 2002 (from the PTHBV data base; Section 2.3). The accuracy of the resulting runoff was interpreted in terms of visual agreement with observed runoff as well as three performance indicators: explained variance (R^2), relative accumulated volume error (RVE), and ratio of simulated to observed maximum daily discharge (Q_{max}-ratio).

Besides the whole-year runoff simulation experiment, a second experiment was performed, aimed at assessing how accurately the different sources were able to forecast the spring flood peak in late April and early May (Figure 3). This forecasting experiment comprised the 2-week period April 22 to May 5. For a certain day in this period, the calibrated HBV model was first run from 020101 (using the same initial state as in the whole-year simulations above) to the previous day, using each of the different sources as input. Thus, at the time of the forecast, the different sources were associated with different HBV model states. Then (the same) actual 2-day forecast from the HIRLAM model was used as input, and a 2-day forecast run was performed. The HIRLAM forecast was produced by an earlier version of the model than described in Section 2.1, having a 44×44 km resolution, and the forecast precipitation input was specified on subbasin level. Overall forecast accuracy was specified in terms of the mean absolute error over the 2-week period, for both 1 day and 2 days ahead forecasts.

4 RESULTS: PRECIPITATION

4.1 Temporal

All temporal analyses were performed using the mean areal precipitation over the entire study area. In Appendix 1, daily time series of mean areal precipitation from each source are shown.

In Table 1, descriptive statistics of the total time series of daily mean areal precipitation from all sources are shown. In terms of total precipitation, the values from HIRLAM, PTHBV and RADAR are all in the range 565-570 mm, whereas the values from the mesoscale analysis are significantly lower, especially the real-time MA22. One obvious reason that MA22 and MA11 are lower than PTHBV is

that the latter has been corrected for observation losses, as mentioned in Section 2.3. This correction may explain the difference between MA11 and PTHBV. The fact that MA22 is lower than MA11 further indicates that rainfall amounts are underestimated in the synoptical observations, as the main difference between MA22 and MA11 is that in the latter corrected data from climate stations are taken into account (Section 2.4).

Table 1. Temporal statistics of daily mean areal precipitation, all 2002.

	HIRLAM	MA22	MA11	PTHBV	RADAR
Total (mm)	566	434	473	565	569
St.dev. (mm)	2.48	2.15	2.30	2.80	2.19
Max (mm)	21.7	15.7	16.9	20.2	11.7
Dry (%)	20.2	42.8	45.0	45.3	21.0

Daily variability, as represented by the standard deviation, is clearly highest for PTHBV, followed by HIRLAM. The lower variability of MA22 and MA11 is possibly related to a generally lower level of precipitation amounts, as indicated in the 2002 totals.

The maximum value is generally rather close to 20 mm, the main exception being radar with only 11.7 mm. This indicates an underestimation by RADAR of large, areally extended rainfalls, which has also been found in e.g. Michelson et al. (2000). Blocking effects is one possible cause, and this under-estimation is likely also a reason for the low standard deviation in the RADAR data, found above.

The percentage of dry days, defined as having a mean areal precipitation less than 0.1 mm, is ~45% for MA22, MA11 and PTHBV, but only ~20% for HIRLAM and RADAR. In the case of HIRLAM, this indicates that the model generates small amounts of precipitation too often. This is a known tendency of HIRLAM/NWP models. The low value for RADAR similarly may indicate a frequent overestimation of light precipitation, but may also be related to the higher areal resolution of RADAR and thus the possibility of detecting precipitation missed by gauges.

The autocorrelation of daily mean areal precipitation from all sources during 2002 are shown in Figure 4. Overall the curves agree rather well, but in almost the entire range of lags (1-14 days) the highest correlation is found in the MA22 series and the lowest in HIRLAM. The low autocorrelation in HIRLAM can be interpreted as an excessive difference between consecutive days' forecasts. It should be mentioned that the deterministic +30h precipitation forecast over an area of the size of the present catchment is known to be of limited accuracy. There does not appear to be any obvious reason for the high autocorrelation in the mesoscale analysis data, MA22 in particular. Rather the difference between HIRLAM and MA22 appears somewhat contradictory, as the latter utilises the former as first guess. This fact is, however, possibly reflected in the similar shapes of the curves (see especially lags 6-8 and 11-13).

For a series with 365 values, the upper confidence limit of the autocorrelation is ~0.1, i.e., correlations below 0.1 are not significantly different from zero correlation (e.g., Haan, 1977). Using this limit, HIRLAM becomes decorrelated at 3 days, RADAR at 4, PTHBV, MA11 at 5, and MA22 at 6 days.

Turning to seasonal analysis, monthly precipitation from all sources are shown in Figure 5. The main deviation from the common pattern is found in the HIRLAM data. For HIRLAM, the precipitation in spring (March-April) is substantially higher than for other sources. In Appendix 1 it can be seen that in March and especially in April HIRLAM generates a small amount of precipitation virtually every day, many of which were dry in the other sources. This confirms the indication from the percentage of dry days above (Table 1). The summer maximum in HIRLAM is shifted one month forward, to July as compared with June for the other sources. In June HIRLAM is consistently low, especially in the last rainy days of the month, whereas in July HIRLAM forecasted a heavy event not observed in the other sources (Appendix 1). Also in autumn HIRLAM stands out, with a September peak not present for the other sources. This peak is due to a number of forecasted high rainfalls that were never observed (Appendix 1).

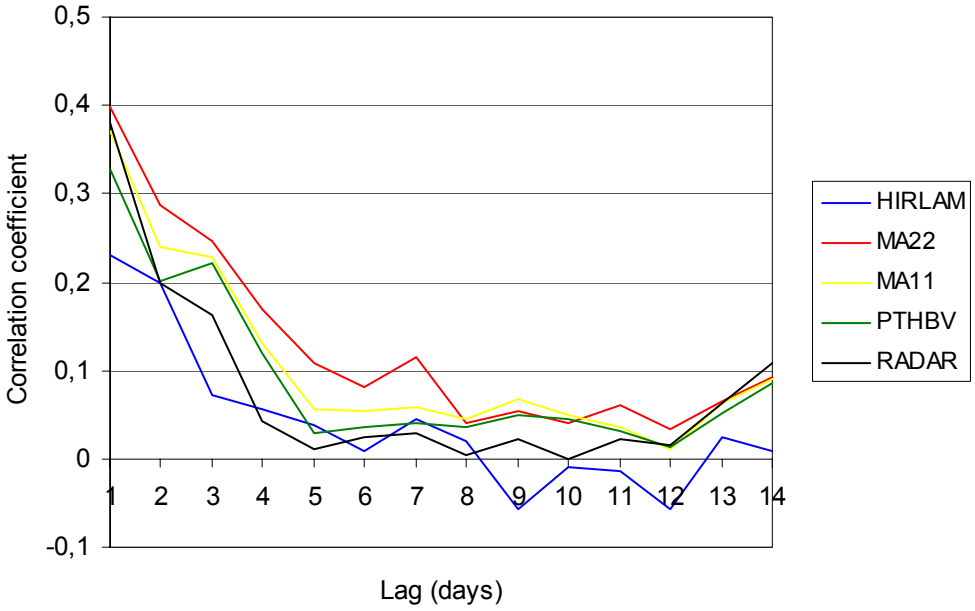

Figure 4. Autocorrelation of daily mean areal precipitation, all 2002.

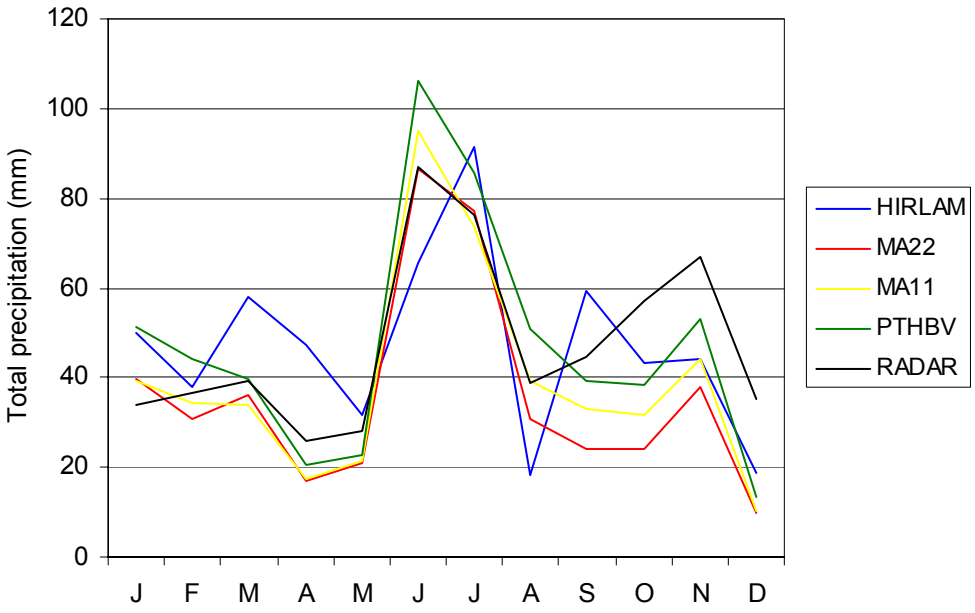

Figure 5. Monthly sums of daily mean areal precipitation.

The overall pattern of the remaining sources agree rather well with a general decrease from January to April, a pronounced summer peak in mainly June but also July, and a smaller peak in November. In terms of amounts, MA22 is consistently low. In spring, as mentioned above, HIRLAM produces the highest values, whereas in summer PTHBV dominates. In autumn there is a notable spread among all sources with a consistent difference of ~35 mm between the highest (generally RADAR) and the lowest (MA22). In the daily time series (Appendix 1), it may be observed that for every day in the period October-December RADAR indicates a rainfall of ~1 mm or more. Whereas HIRLAM and RADAR are variable, there is throughout the year (most clearly during autumn) a consistent pattern with PTHBV>MA11>MA22, which is reflected in the common shape of the curves in Figure 5.

If looking back at Table 1, the striking agreement in total precipitation between HIRLAM, PTHBV and RADAR thus appears to be rather coincidental. As compared with PTHBV, the annual pattern of HIRLAM is quite different, whereas RADAR underestimates summer and overestimates autumn precipitation (see Appendix 1). On the other hand, the lower values of MA11 and in particular MA22 (Table 1) are caused by systematically lower rainfall amounts during the entire year, which is in line with the suggested reasons.

In Figure 6, the temporal standard deviation during individual months are displayed. As in the case of monthly precipitation amounts (Figure 5), HIRLAM stands out from the rest. This happens especially during summer when HIRLAM displays a reversed pattern, in particular in comparison with PTHBV. An inspection of the daily series (Appendix 1) shows that the high value of HIRLAM in July is largely due to the high event mentioned above in connection with Figure 5, whereas the low standard deviation in August is due to a systematical underestimation. The high value of PTHBV in August is largely due to one single event (Appendix 1).

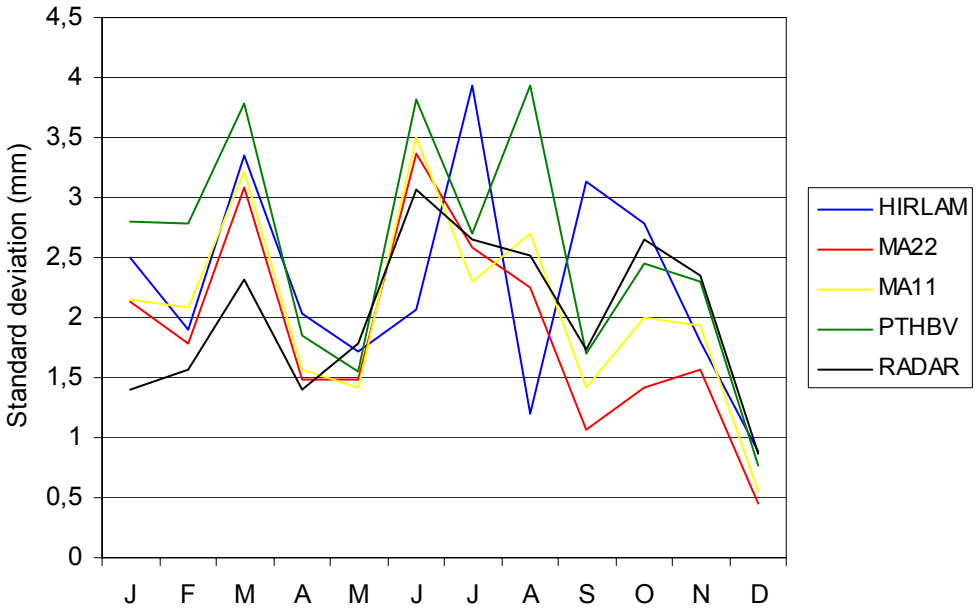

Figure 6. Monthly mean standard deviation of daily mean areal precipitation.

The variation of maximum daily mean areal precipitation in each month (Figure 7) resembles the annual variation in standard deviation shown in Figure 6. Most remarkable in Figure 7 are the peaks of HIRLAM and PTHBV in July and August, respectively, which both have been commented above in connection with Figures 5 and 6. Inspection of the daily series (Appendix 1) confirms that, as expected, the different sources' maxima generally occurs on the same day in the month. Exceptions from this rule occur mainly for HIRLAM, which sometimes generate maxima on days different from the other sources (see April, May, July, September in Appendix 1).

4.2 Areal

All areal analyses were performed for the 20 grid nodes corresponding to a 22×22 km resolution (see Section 2.5). The areal distributions of 2002 total precipitation from each source are shown in Appendix 2.

A visual inspection of the maps in Appendix 2 reveals a rather complex pattern, which further differs between sources. The "gauge-derived" sources (PTHBV, MA22, MA11) all indicate a precipitation maximum in the south-west corner of the area, and a minimum in the north-west corner. Whereas the mesoscale analysis indicate a minimum in south-east, PTHBV shows a high precipitation in the entire eastern part of the area. The gradient in mean altitude from ~300 m.a.s.l. in the east to ~400 m.a.s.l. in

the west implies a general increase in the precipitation from east to west. This tendency is suggested in MA22 and MA11.

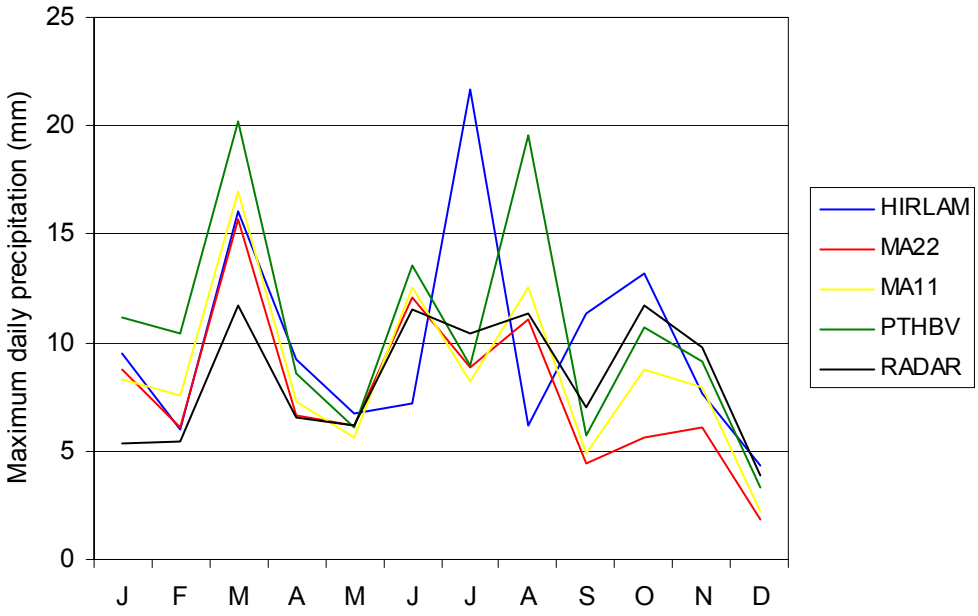

Figure 7. Monthly maximum daily mean areal precipitation.

Table 2 contains the areal standard deviations for each source during the entire year. The top row shows the standard deviation of the 2002 totals in each of the 20 grid nodes (shown in the maps of Appendix 2). MA22, MA11 and PTHBV all agree well with values around 20-25 mm. HIRLAM is markedly higher with almost 50 mm, and RADAR is almost 10 times higher with over 200 mm. An inspection of the maps (Appendix 2) shows that the high standard deviation in RADAR is caused mainly by two grid nodes in the north-west corner with annual totals of 760 mm and 1390 mm, respectively, as compared with a mean total of 515 mm in the remaining 18 nodes. For these 18 nodes, the standard deviation is 48.3 mm, i.e., similar to HIRLAM. Apparently rainfall amounts are systematically overestimated by the radar over a limited region in the north-west, and further investigation of this inhomogeneity is made below.

Table 2. Areal standard deviation of precipitation, all 2002.

	HIRLAM	MA22	MA11	PTHBV	RADAR
2002 total (mm)	47.3	26.7	21.2	21.0	205.9
Mean daily (mm)	0.749	0.966	1.103	1.094	1.367

The bottom row in Table 2 shows the mean standard deviation of daily fields. Again MA22, MA11 and PTHBV agree well, this time all are close to 1 mm. RADAR is substantially higher at almost 1.4 mm, which is likely much related to the local overestimation found above. The high value for RADAR may also be related to the higher level of detail in the original radar data, which may affect also the areal averages. Interestingly, on a daily basis the areal variability in the HIRLAM fields is lower than that of MA22, MA11 and PTHBV, in contrast with the opposite situation found for the 2002 total. Thus, whereas areal variability is smoothed on a daily basis, there is a stronger geographical dependency in the HIRLAM data as compared with gauge data. This may be due to that orography in the model induces small but systematic variations in areal precipitation, that summed up over a year makes a significant contribution.

The monthly variation of the mean areal standard deviation is shown in Figure 8. The overall pattern is a seasonal cycle with a distinct peak in summer, when convective, local events give rise to a

pronounced areal variability, and lower values from autumn to spring, when larger-scale systems produce most of the precipitation.

From January to July all sources agree well, except for consistently lower values for HIRLAM. In August there is a very wide spread among the sources, but this month is associated with a high uncertainty as there were only a few significant precipitation events, which were further very areally inhomogeneous. From September to December all sources again agree well, the exception now being RADAR which exhibits very high values from October to December. An inspection of the data reveals that the high standard deviation is caused mainly by one node in the averaged grid, which consistently registered a high rainfall in the period, on average ~9 mm/day which is almost 8 mm higher than the mean precipitation in other grid nodes. This also explains the high mean precipitation registered by RADAR during October-December (Figure 5), and the high areal standard deviation in the grid nodes' 2002 total (Table 2). Thus the inhomogeneity in the RADAR data appear to be localised not only in space (1-2 grid nodes, corresponding to 500-1000 km²) but also in time (October-December). It may be added that range-dependent biases in the RADAR data are known to be most pronounced during autumn and winter.

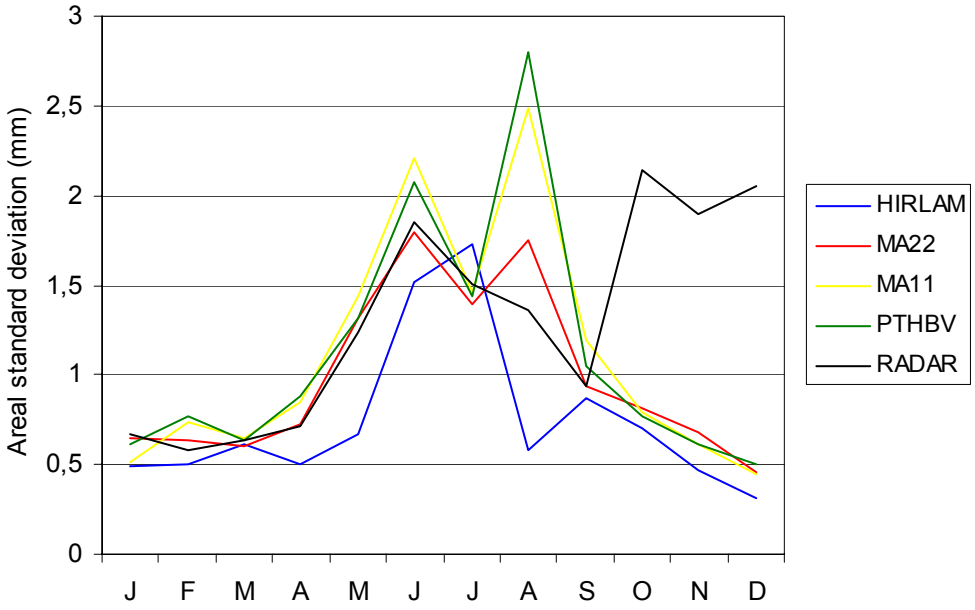

Figure 8. Monthly mean areal standard deviation.

The variation of correlation with distance for all sources are shown in Figure 9. In all cases the correlation appears to decrease nearly linearly with distance. The highest correlation coefficient is exhibited by PTHBV (lag<75 km) and HIRLAM (lag>75 km). The high correlation for HIRLAM is likely caused by areal smoothing in the model design. For MA22, MA11 and PTHBV, the curves in Figure 9 reflect the areal smoothing related to the structure functions used in the optimal interpolation procedure (e.g., Häggmark et al., 1997). The fact that MA22 exhibits a higher correlation coefficient than MA11 may reflect that the former uses HIRLAM as first guess in the optimal interpolation. Overall, HIRLAM, MA22, MA11 and PTHBV are rather similar and it is difficult to find clear explanations for the small differences observed (also in light of the areal integration performed). However, RADAR clearly and consistently exhibits the lowest correlation. This is, at least partly, owing to the inhomogeneity problem discussed in connection with Figure 8 above.

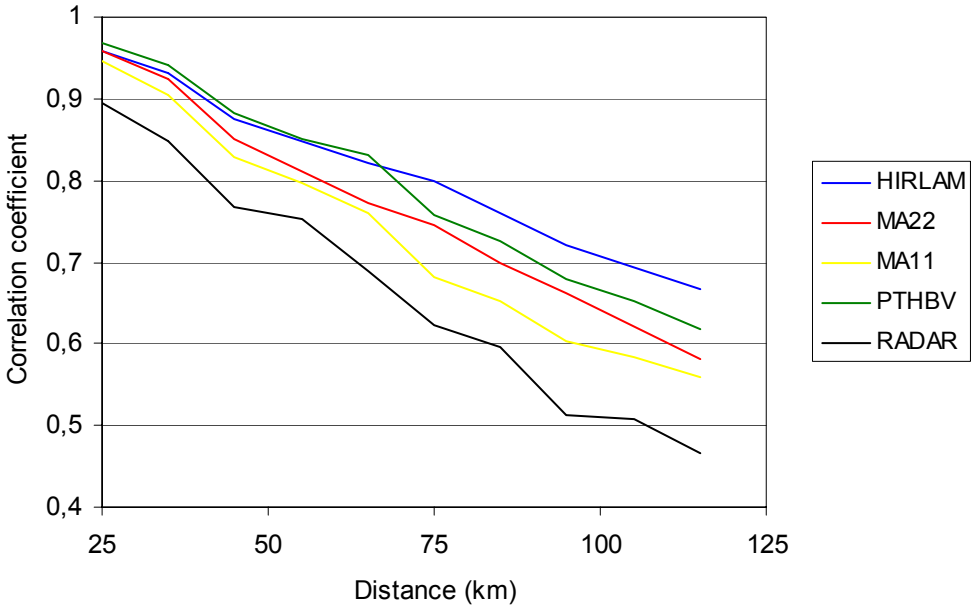

Figure 9. Areal correlation of daily precipitation, all 2002.

5 RESULTS: RUNOFF

5.1 Gimdalsbyn

Figure 10 shows observed runoff during 2002 in station Gimdalsbyn, and simulated runoff obtained using PTHBV, HIRLAM and RADAR, respectively, as input. The result from sources MA22 and MA11 are shown in Appendix 3, where all results for Gimdalsbyn are displayed together with the corresponding precipitation input.

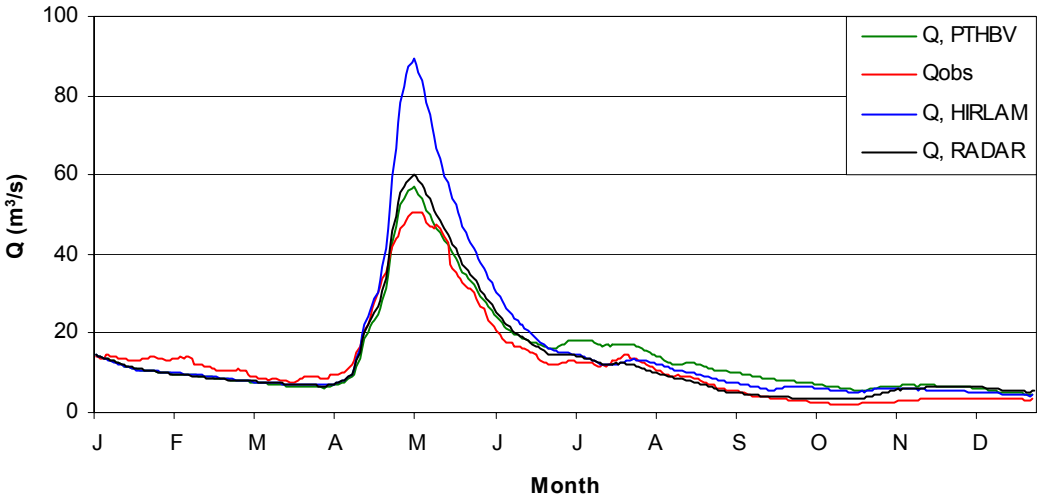

Figure 10. Observed and simulated runoff in station Gimdalsbyn during 2002.

As expected, all sources well reproduce the overall intra-annual discharge pattern. In the period January-March, all sources weakly underestimate the discharge. The spring flood is overestimated to various degrees by three sources (HIRLAM, RADAR, PTHBV) and weakly underestimated by the other two (MA22, MA11). During the second half of the year discharge is weakly overestimated by all sources.

The most striking difference compared with observations is the spring flood generated from HIRLAM, with a peak value that exceeds the observed by 40 m³/s. An analysis of the simulation runs revealed that the main source of this discrepancy is the overestimated precipitation by HIRLAM in March and (mainly) April (see Figure 5 and Appendix 1). In March, the overestimated precipitation by HIRLAM produced a snow depth approximately 20 mm (water equivalent) larger than PTHBV. Snow melt occurred almost exactly within April (i.e., started April 1 and finished April 30), but in reality this melt was not accompanied by any significant precipitation, except for the last days in April and first days in May. HIRLAM, however, generated a small amount of precipitation (~1 mm) almost every day in April. These small but frequent additions, in combination with some overestimation of the heavy precipitation in late April and early May, were the reasons for the overestimated spring flood.

Another difference worth commenting is the overestimated runoff in summer and autumn by PTHBV. Generally the high runoff is caused by a high precipitation, as seen in Figure 5 PTHBV has the highest precipitation of all sources in summer. Still, as PTHBV has been used in the calibration, it could be expected that this difference between sources would result in an underestimation of runoff by the other sources, rather than an overestimation by PTHBV. However, as seen in Figure 2a the low-flow periods are virtually always more or less inaccurately reproduced. Sometimes observed discharge is overestimated, sometimes underestimated. This may be partly related to the automatic calibration routine in which model parameters related to the simulation of high flow were calibrated (and fixed) before parameters related to low flow, i.e., more weight was given to reproduction of runoff peaks than of base flow. It is possible that manual calibration could have improved performance in this respect, but we chose automatic calibration for reasons of consistency and objectivity.

It may further be noted that the inhomogeneities found in the RADAR precipitation did not have any clear negative impact on the simulated runoff, but overall the accuracy of RADAR simulated runoff is comparable to that of PTHBV. The inhomogeneities were, however, limited in space to a small and remote part of the subbasin (Appendix 4) and in time to the (base flow) period October-December (in Figure 10 some overestimation of the base flow by RADAR is apparent during October-December).

Table 3 summarises the runoff simulations in terms of the three performance indicators explained variance (R^2), relative accumulated volume error (RVE), and ratio of simulated to observed maximum daily discharge (Q_{max}-ratio). In terms of all three indicators, the best performance is achieved by MA11 (see also Appendix 3), despite the underestimation of 2002 total precipitation, as compared with PTHBV (Table 1). The even more pronounced underestimation of MA22 precipitation leads to underestimations of runoff in terms of both accumulated volume and peak discharge. For HIRLAM, PTHBV and RADAR, the indicators reflect the features in Figure 10 discussed above.

Table 3. Runoff simulation performance for station Gimdalsbyn.

	HIRLAM	MA22	MA11	PTHBV	RADAR
R^2	0.49	0.93	0.96	0.91	0.94
RVE (%)	26	-11	-3	14	6
Q_{max}-ratio	1.78	0.84	0.94	1.13	1.20

Figure 11 shows a typical result from the forecasting experiment at station Gimdalsbyn. Source MA22 produces the most accurate forecasts, only a slight underestimation of the observed discharge. For source MA22 the underestimation is more pronounced. RADAR and PTHBV overestimate the runoff somewhat by approximately the same amount, whereas source HIRLAM generates substantial overestimations, in line with the results in Figure 10.

The result for all days in the 2-week period April 22 to May 5 are shown in Appendix 5, and it is clear that throughout the period the pattern in Figure 11 prevails. The only notable deviation is that in the end of the period the underestimation by MA11 becomes more pronounced, which makes the PTHBV and RADAR forecasts the most accurate for the last few days. Overall it is obvious that the forecast performance is very much given by the discharge level at the start of the forecast period, as the rainfall amounts during the period (Appendix 1) are not large enough to have any substantial impact on the snow-melt dominated runoff.

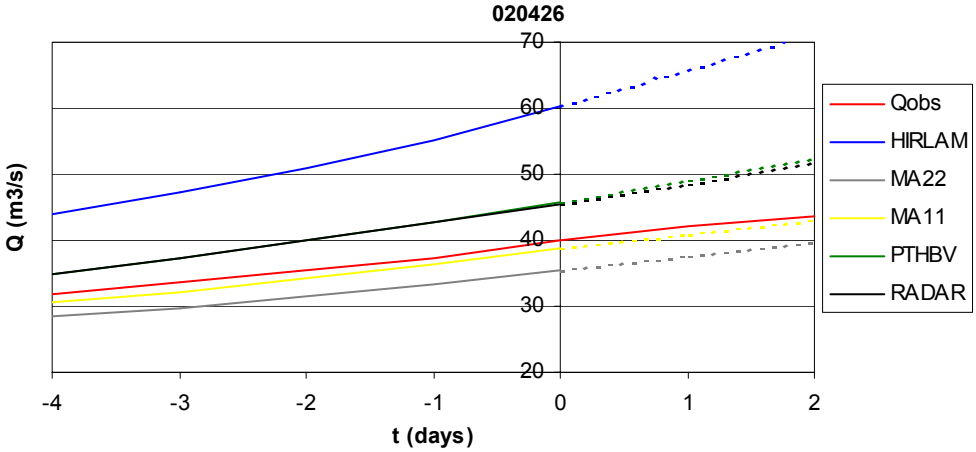

Figure 11. 2-days runoff forecasts at station Gimdalsbyn on April 26 (t=0).

Table 4 shows the mean absolute error over the forecast experiment period for 1- and 2-day forecasts. The values in the table confirm the above findings, i.e., that MA11 is clearly superior with mean absolute error of less than 3 m³/s, MA22, PTHBV and RADAR have a similar and somewhat higher error of ~7 m³/s, and HIRLAM exhibits the highest error of almost 30 m³/s. The difference in accuracy between the 1-day and 2-day forecast is small.

Table 4. Mean absolute error (m³/s) in forecasting experiment for station Gimdalsbyn.

	HIRLAM	MA22	MA11	PTHBV	RADAR
Day 1	26.9	6.1	2.6	7.2	6.6
Day 2	28.1	6.5	2.9	7.4	6.8

5.2 Torpshammar

Figure 12 shows the observed and simulated runoff for station Torpshammar, i.e., the outlet of the entire catchment, and overall the picture is similar to that of station Gimdalsbyn above.

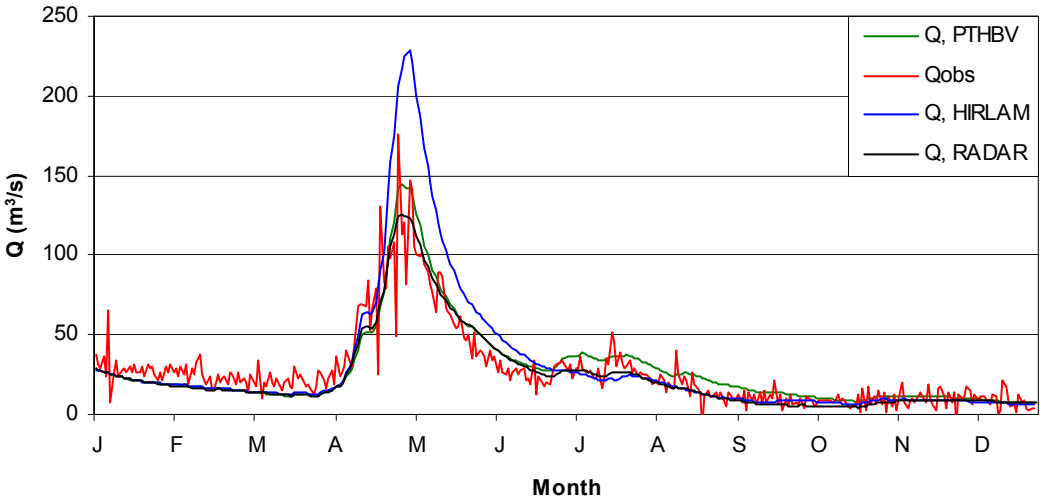

Figure 12. Observed and simulated runoff in station Torpshammar during 2002.

As for Gimdalsbyn, all sources slightly underestimate the runoff in the period January-March, HIRLAM overestimates the spring flood, and PTHBV slightly overestimates the runoff in summer. Any influence of the overestimated precipitation by RADAR in October-December is not noticeable for the entire catchment. MA22 and MA11 generally perform well (Appendix 4), similarly to

RADAR, but the low amount of precipitation estimated by MA22 in the period September-December (Figure 5) is reflected in a clear underestimation of runoff in this period.

Table 5 summarises the runoff simulations in terms of the three performance indicators. The consistently lower value of R^2 as compared with station Gimdalsbyn is partly a numerical consequence of the irregular appearance of the observed runoff. This irregularity further makes Q_{max}-ratio less useful as performance indicator. Nevertheless, the overall best performance for the entire catchment is found for PTHBV. Sources MA22, MA11 and RADAR all have a slightly higher R^2, but both accumulated and peak runoff are clearly underestimated. Naturally, this is related to the fact that calibration was performed for PTHBV.

Table 5. Runoff simulation performance for station Torpshammar.

	HIRLAM	MA22	MA11	PTHBV	RADAR
R^2	0.20	0.81	0.83	0.79	0.83
RVE (%)	14	-20	-14	-3	-10
Q_{max}-ratio	1.30	0.65	0.67	0.82	0.71

Owing to the strong variability of the observed discharge at station Torpshammar, in particular at the time of the spring flood peak (Figure 3), the results of the forecast experiment varied widely from day to day, in contrast with the regular behaviour at station Gimdalsbyn (Appendix 2). Figure 13 shows an example of the result from station Torpshammar, on April 28, one day before the spring flood peak maximum of 176 m³/s. Concerning the 1-day ahead forecast, HIRLAM overestimates and PTHBV underestimates the flood peak by the same amount (~25 m³/s), whereas all other sources underestimate the peak by more than 50 m³/s. Concerning the 2-day ahead forecast, however, all sources overestimate the observed runoff, HIRLAM by almost 100 m³/s and MA22 by only 5 m³/s.

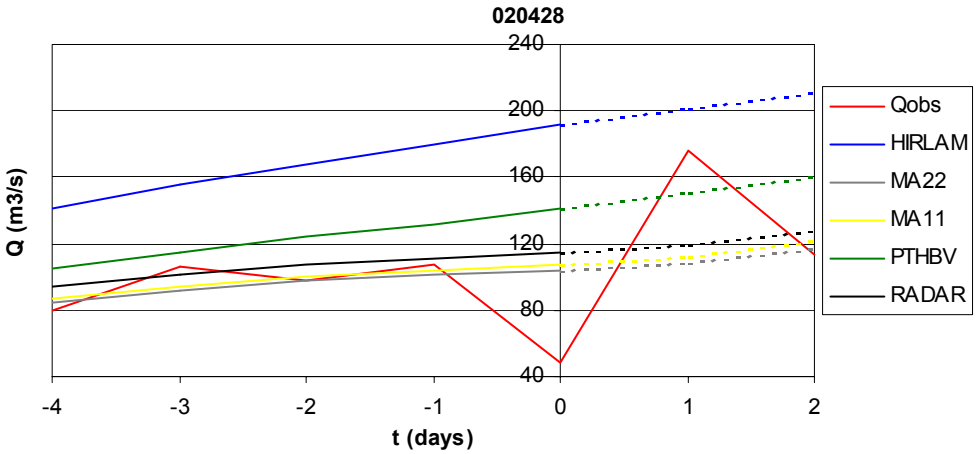

Figure 13. 2-days runoff forecasts at station Torpshammar on April 28 (t=0).

The result for all days in the 2-week period are shown in Appendix 6. As for station Gimdalsbyn, the forecasts are very regular owing to the snow-melt dominance, constantly reflecting the discharge level at the start of the forecast period. As mentioned above, the accuracy of the various sources varies from day to day and no source is clearly superior. This is confirmed Table 6, showing the mean absolute errors over the experiment period. Due to the variability of the observations the overall error levels are clearly higher than for station Gimdalsbyn. Sources MA11, MA22 and RADAR all have a similar mean error of ~20 m³/s, PTHBV a somewhat larger error of ~30 m³/s, and HIRLAM a markedly larger of ~75 m³/s. As for station Gimdalsbyn, the error difference between the 1-day and 2-day forecasts is remarkably low.

Table 6. Mean absolute error (m^3/s) in forecasting experiment for station Torpshammar.

	HIRLAM	MA22	MA11	PTHBV	RADAR
Day 1	75.4	21.9	20.0	29.3	19.7
Day 2	77.6	22.5	20.8	31.7	20.4

6 SUMMARY AND CONCLUSIONS

In the first step of this analysis, daily precipitation during 2002 over catchment Gimån, central Sweden, from five sources - NWP model (HIRLAM), radar (RADAR), gauges (PTHBV), mesoscale analysis (two versions; MA11 and MA22) - were compared in search of systematic differences. In the second step, areal precipitation estimates from the different sources were used to drive the hydrological HBV model, to assess the effect of the differences between the sources in runoff simulation and hydrological forecasting.

The main observations from the comparison of areal precipitation were the following:

- The mesoscale analysis consistently generated the lowest amount of precipitation, leading to a difference of ~100 mm for total precipitation over the area in 2002. This may be due to partly that correction for observation losses is not performed, and partly an underestimation of rainfall amounts in synoptical observations.
- The seasonal cycle of precipitation in HIRLAM differed somewhat from the other sources, although the overall pattern agreed fairly well. Notable were an overestimation of spring rainfall (due to many forecasted small rainfalls never observed) and an underestimation of summer rainfall (due to forecasted but underestimated high rainfalls).
- Throughout the year and especially in autumn, the mean areal precipitation amounts generally follow the order PTHBV>MA11>MA22, which can be explained similarly to the first item above, whereas HIRLAM and RADAR are more variable.
- The areal standard deviation in the HIRLAM data was low on a daily basis but high for the 2002 totals. Areal smoothing in the model may explain the low daily areal variability, whereas the high areal variability of annual totals may originate from orographically induced small but systematic areal variations.
- In the RADAR data a distinct inhomogeneity was found, with precipitation amounts being consistently overestimated by ~8 mm/day over a region of 500-1000 km² (as estimated from the coarse, averaged grid) during October-December. The source of this problem has not been possible to identify during this study, we can only speculate that it is related to temporally improper functionality of the Östersund radar, north-west of the study catchment.
- Areal correlation decreased nearly linearly for all sources, with the highest correlation coefficients in HIRLAM and PTHBV, and the lowest in RADAR.

Overall the data from HIRLAM and RADAR agreed reasonably well with the other, "gauge-derived" sources, but the present comparison highlighted some differences. In HIRLAM, the seasonal cycle differed somewhat. This difference is possibly of a systematic character, judging from the 2002 data, but longer series are required to verify it. The different tendencies of the areal variability in the HIRLAM fields on a short-term (daily; low variability) and a long-term (annual; high variability) basis, respectively, may deserve further investigation. The temporal and areal inhomogeneities found in the RADAR data also require further analysis to identify the source of the problem and to improve the applicability for, e.g., hydrological forecasting.

The main observations from the comparison of simulated and forecasted runoff were the following:

- Basin runoff during 2002 was characterised by a pronounced spring flood in the period April-June, reaching its peak in early May, and a rather stable discharge during the rest of the year.
- HBV model calibration was performed using PTHBV data, but this did not result in a significantly better performance for PTHBV than the other sources in 2002.
- HIRLAM substantially overestimated the spring flood. This was mainly because HIRLAM generated small amounts of precipitation almost every day in April, many of which in reality were

dry, at the same time as snow melt occurred. HIRLAM further overpredicted some high rainfalls in the end of the snow-melt period.
- PTHBV overestimated runoff in summer and early autumn, in line with the high estimated precipitation by PTHBV during this period. This may partly be related to calibration strategy.
- The inhomogeneities found in the RADAR precipitation did not have a strong impact on simulated runoff, mainly because they only affected a small part of the catchment and occurred in a period with near base-flow conditions.
- MA22 and MA11 both performed well in the runoff simulations, especially for the western subbasin (station Gimdalsbyn), but the low amounts of precipitation resulted in underestimations of both accumulated and peak runoff.
- As the spring flood peak was largely dominated by snow melt, the performance of the various sources in forecasting the peak runoff was governed more by the model state before the peak than by the estimated precipitation around the time of the peak. In the case of station Torpshammar, the high variability of observed runoff made it difficult to assess the forecasting performance of the various sources.
- As in the simulation, HIRLAM substantially overestimated the spring flood peak also in the forecasting experiment. The accuracy of the other sources were similar, although MA11 performed somewhat better than the other at station Gimdalsbyn and PTHBV somewhat worse than the other at station Torpshammar.

Besides the striking overestimation of spring flood by HIRLAM, all sources performed rather similarly in the runoff simulation, with only minor differences which mainly reflected the differences in areal precipitation estimates. It must be emphasised that in comparatively large catchments such as the one used here, with a long response time, differences in the spatial distribution of precipitation tend to even out and not be much reflected in the catchment runoff. Spatial smoothing is further required by the structure of the HBV model, which uses as input precipitation averaged over subbasins. Moreover, the runoff in 2002 was normal without challenging floods or droughts that could possibly have separated the sources better. Future tests of the performance of different precipitation sources (especially RADAR) will focus on smaller catchments during periods of flooding.

Finally we wish to emphasise that this is a case study - observations made and conclusions drawn are strictly valid only for the specific time period and region under investigation. Concerning time, one year is clearly not enough for a proper long-term assessment of systematic differences between sources. On the other hand, as both models and analysis systems are under constant development, it may simply be practically difficult (or even impossible) to obtain consistent historical output for all sources during longer time periods (at least it was not possible within the scope of the present study). Concerning area, the size of the study region is rather small, especially in relation to the 22×22 km resolution of HIRLAM and MA22. Further, the temporal and areal representativity of a certain time period and region is always to some extent unknown, but it is clear that in the present case neither time period nor region represents any extreme conditions. Nevertheless, further investigations are required to judge to which degree the results obtained in the present study can be generalised.

Acknowledgements

We are most grateful to Nils Gustafsson, Günther Haase, Anna Jansson, Tomas Landelius, Magnus Lindskog and Daniel Michelson, all at SMHI, for help with data extraction and preparation as well as fruitful discussions.

References

Arheimer, B., 1998. Riverine Nitrogen – analysis and modelling under Nordic conditions. Ph.D. thesis, Kanaltryckeriet, Motala. pp. 200.

Bergström, S., 1976. Development and application of a conceptual runoff model for Scandinavian catchments. SMHI Reports Hydrology and Oceanography, nr. 7, 134 pp.

Bergström, S., 1992. The HBV model - its structure and applications. SMHI Reports Hydrology, nr. 4, 35 pp.

Bergström, S. and B. Carlsson, 1994. River runoff to the Baltic Sea: 1950-1990. Ambio, 23, 280-287.

Bergström, S., J. Harlin and G. Lindström, 1992. Spillway design floods in Sweden. I: New guidelines. Hydrol. Sci. J., 37, 505-519.
Brandt, M., T. Jutman and H. Alexandersson, 1994. Sveriges Vattenbalans. Årsmedelvärden 1961-1990 av nederbörd, avdunstning och avrinnning. SMHI Hydrologi, nr. 49, 16 pp.
Førland, E.J., P. Allerup, B. Dahlström, E. Elomaa, J. Jonsson, H. Madsen, J. Perälä, P. Rissanan, H. Vedin and F. Vejen, 1996. Manual for operational correction of nordic precipitation data. DNMI Report nr. 24/96, Norwegian Meteorological Institute, Norway, 66 pp.
Graham, P., 1999. Modelling runoff to the Baltic basin. Ambio 28, 328-334.
Haan, C.T., 1977. Statistical methods in hydrology. Iowa State University Press, USA, 378 pp.
Häggmark, L., K-I.Ivarsson and P-O. Olofsson, 1997. MESAN – Mesoscale Analysis (in Swedish). SMHI Reports Meteorology and Climatology, nr. 75, 77 pp.
Häggmark, L., K-I. Ivarsson, S. Gollvik and P-O. Olofsson, 2000. Mesan, an operational mesoscale analysis system. Tellus, 52A, 2-20.
Johansson, B., 2002. Estimation of areal precipitation for hydrological modelling. Ph.D Thesis, Earth Sciences Centre, Göteborg University, Report nr. A76.
Jutman, T., 1992. Production of a new runoff map of Sweden. Proceedings of Nordic Hydrological Conference, 4-6 August, Alta, Norway, NHP report, nr. 30, 643-651.
Koistinen, J. and D.B. Michelson, 2002. BALTEX weather radar-based products and their accuracies. Boreal Env. Res., 7, 253-163.
Koistinen, J. and T. Puhakka, 1981. An improved spatial gauge-radar adjustment technique. Preprints 20th AMS Conf. on Radar Met., Nov. 30-Dec. 3, Boston, MA., 179-186.
Källén, E., 1996. HIRLAM Documentation Manual. Available from SMHI, 60176 Norrköping, Sweden.
Lindström, G., 1997. A simple automatic calibration routine for the HBV Model. Nordic Hydrol., 28, 153-168.
Lindström, G. and A. Rodhe, 1992. Transit times of water in soil lysimeters from modelling of oxygen-18. Water, air and soil pollution, 65, 83-100.
Lindström, G., B. Johansson, M. Persson, M. Gardelin and S. Bergström, 1997. Development and test of the distributed HBV-96 hydrological model. J. Hydrol., 201, 272-288.
Louis, J.F., 1979. A parametric model of vertical eddy fluxes in the atmosphere. Bound.-Layer Meteorol., 17, 187-202.
Michelson D.B., 2003. Systematic correction of precipitation gauge observations using analyzed meteorological variables. J. Hydrol., in press.
Michelson, D.B., T. Andersson, J. Koistinen, C.G. Collier, J. Riedl, J. Szturc, U. Gjertsen, A. Nielsen and S. Overgaard, 2000. BALTEX Radar Data Centre products and their methodologies. SMHI Reports Meteorology and Climatology RMK Nr. 90, SMHI, SE-601 76, Norrköping, Sweden, 76 pp.
Nash, J.E. and J.V. Sutcliffe, 1970. River flow forecasting through conceptual models. Part I - A discussion of principles. J. Hydrol., 10, 282-290.
Press, W.H., S.A. Teukolsky, W.T. Vetterling and B.P. Flannery, 1992. Numerical Recipes in FORTRAN. The Art of Scientific Computing, Second Edition, Cambridge University Press.
Savijärvi, H., 1989. Fast radiation parameterization schemes for mesoscale and short-range forecast models. J. Appl. Meteorol., 29, 437-447.
Sundqvist H., E. Berge and J.E. Kristjansson, 1989. Condensation and cloud parameterization studies with a mesoscale numerical weather prediction model. Mon. Wea. Rev., 117, 1641-1657.
Undén, P., L. Rontu, H. Järvinen, P. Lynch, J. Calvo, G. Cats, J. Cuxart, K. Eerola, C. Fortelius, J. Antonio Garcia-Moya, C. Jones, G. Lenderlink, A. McDonald, R. McGrath, B. Navascues, N. Woetman Nielsen, V. Ødegaard, E. Rodriguez, M. Rummukainen, R. Rõõm, K. Sattler, B. Hansen Sass, H. Savijärvi, B. Wichers Schreur, R. Sigg, H. The and A. Tijm, 2002. HIRLAM-5 Scientific Documentation. HIRLAM-5 Project, c/o Per Undén SMHI, S-601 76 Norrköping, Sweden.
SMHI, 2002. Weather and Water - the Weather Year 2002 (in Swedish), nr. 13, SMHI, SE-601 76, Norrköping, Sweden ,15 pp.

APPENDIX 1 1(4)

Daily time series

January

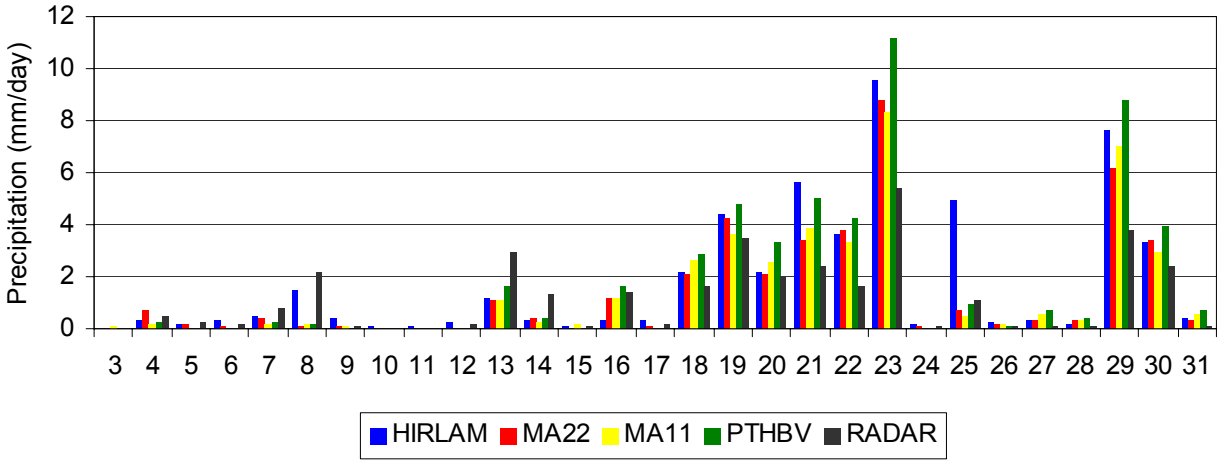

February

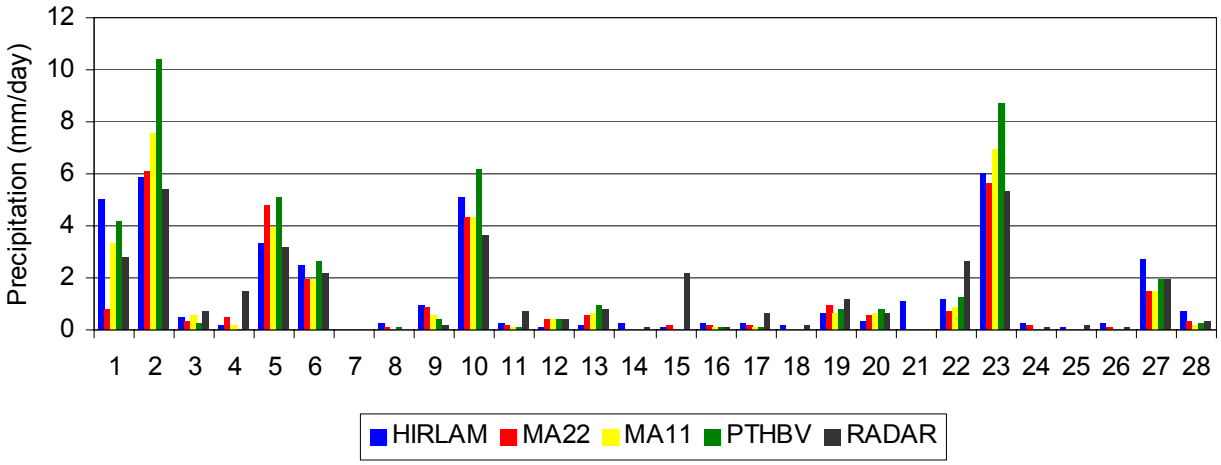

March

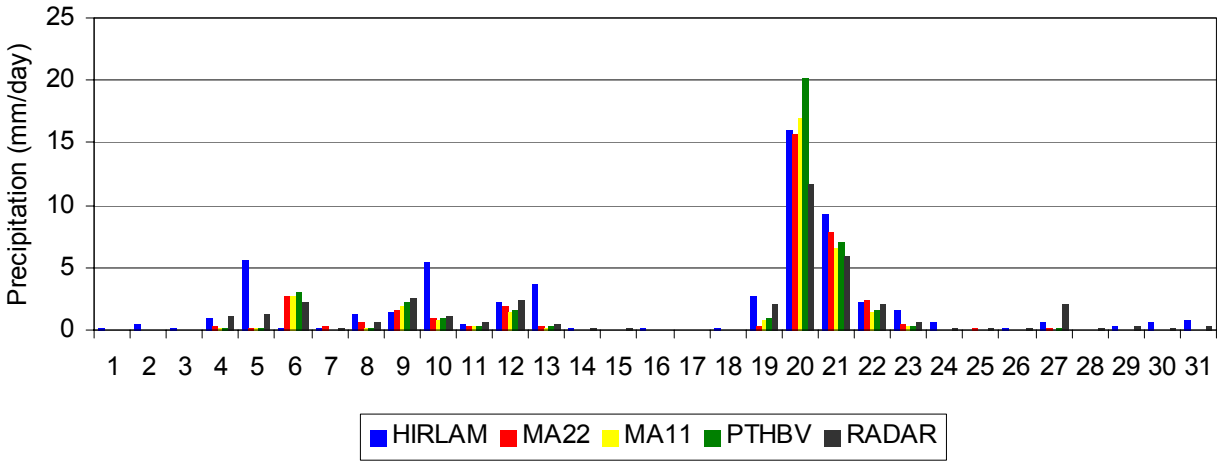

April

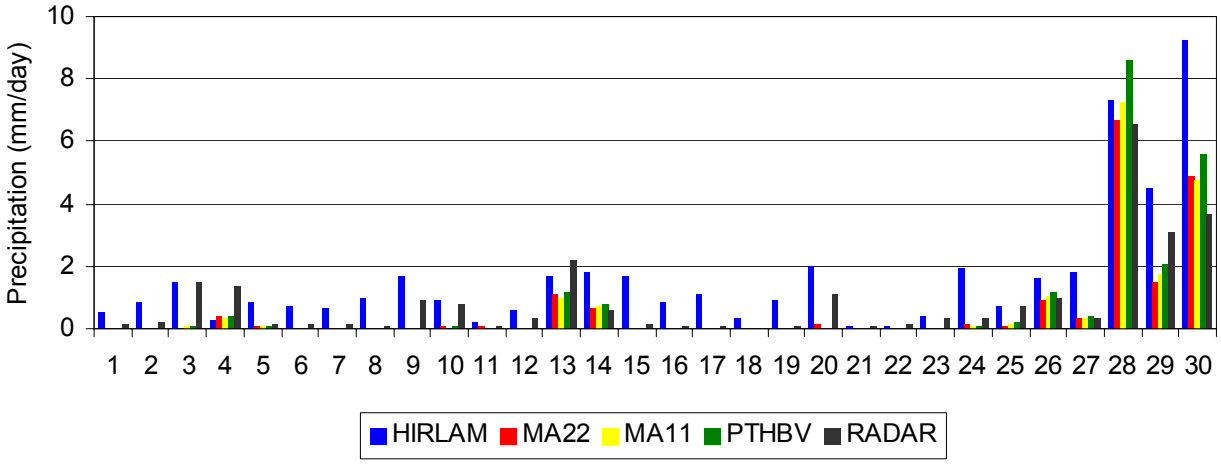

May

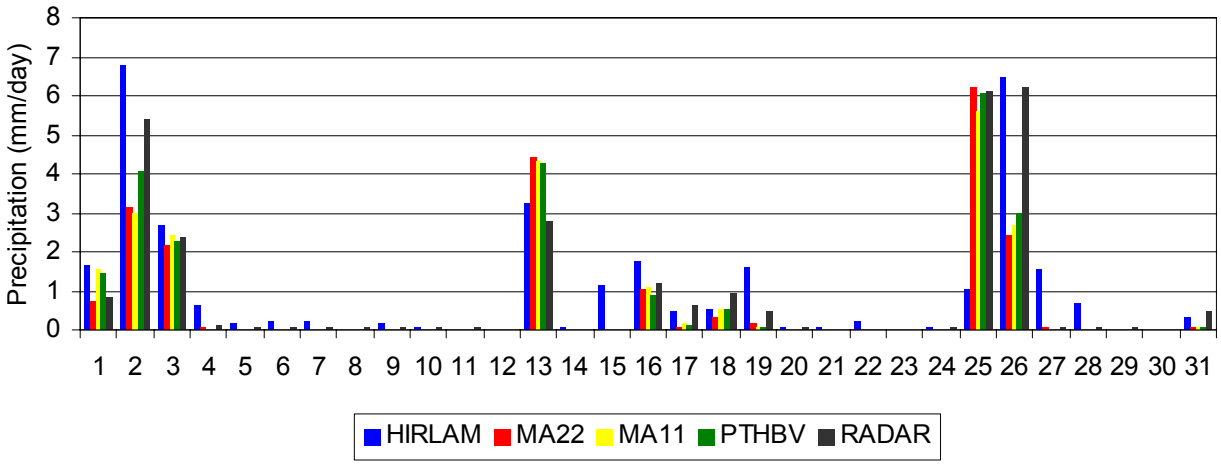

June

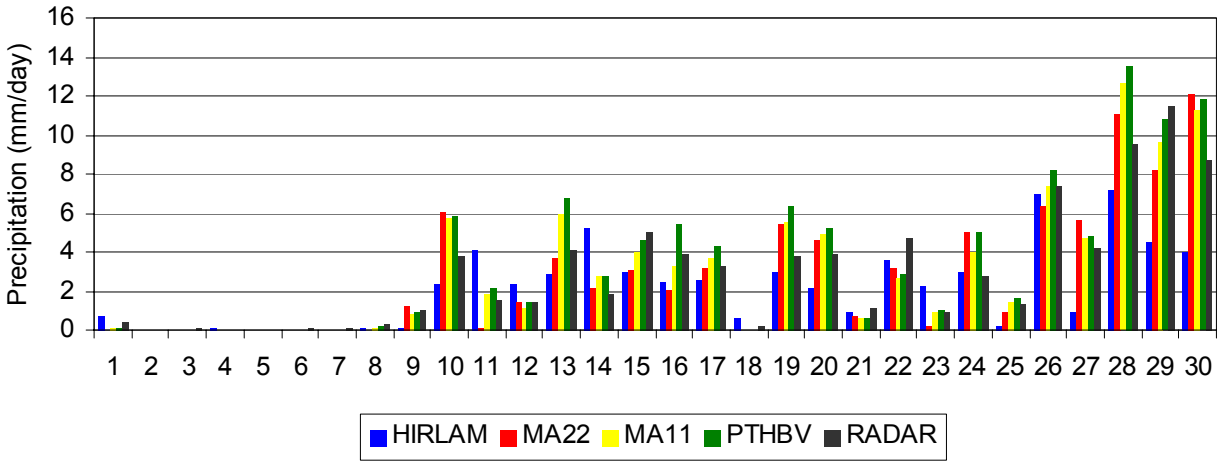

July

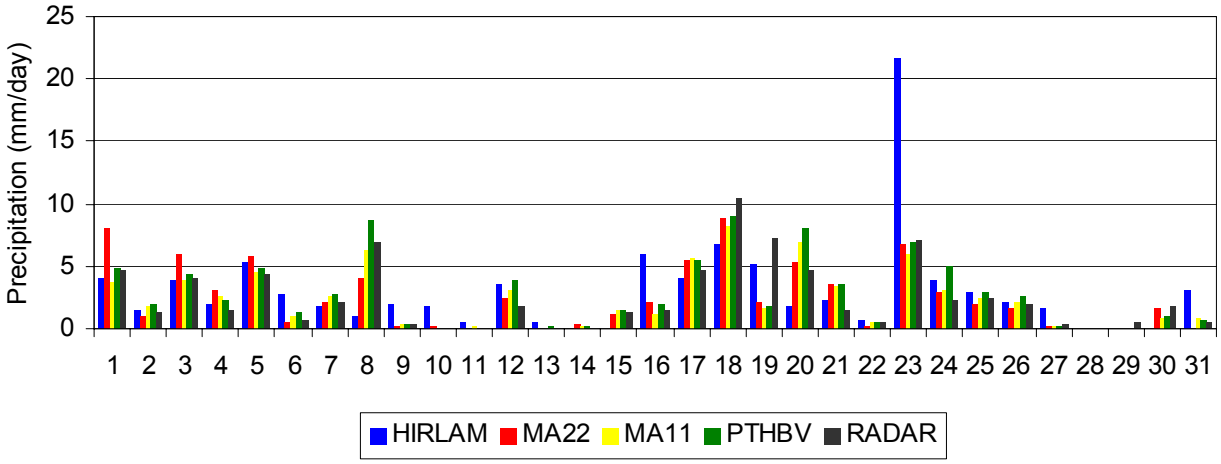

August

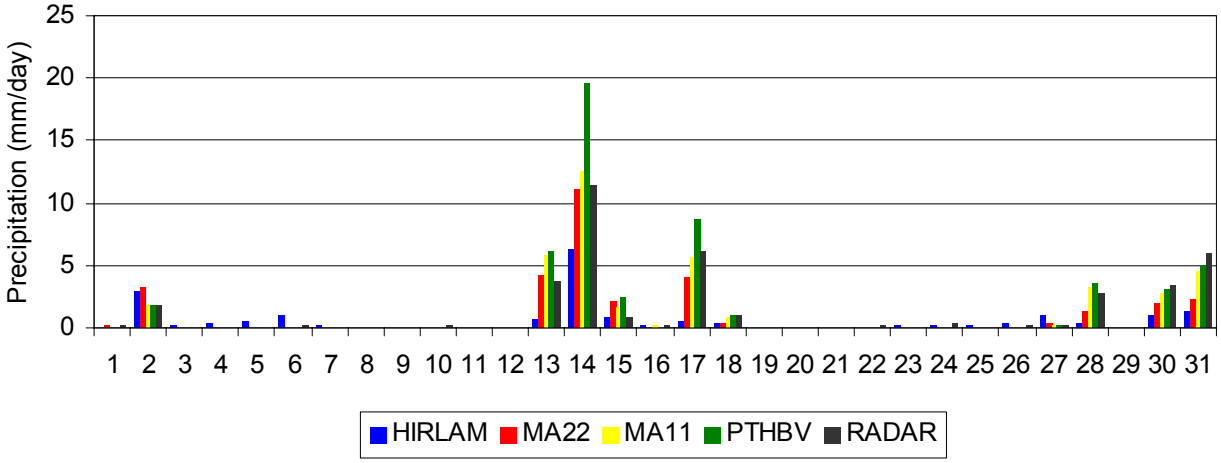

September

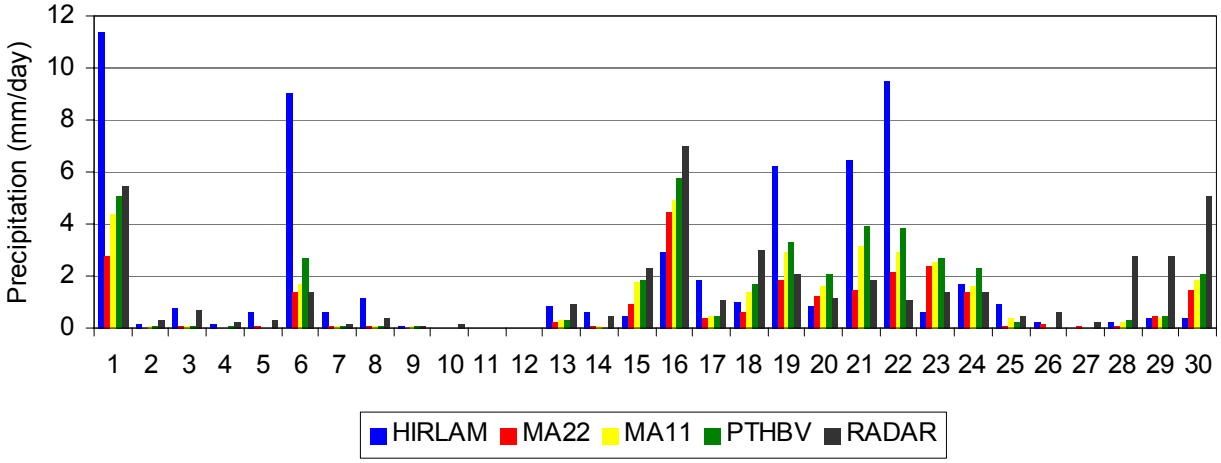

APPENDIX 1 4(4)

Daily time series

October

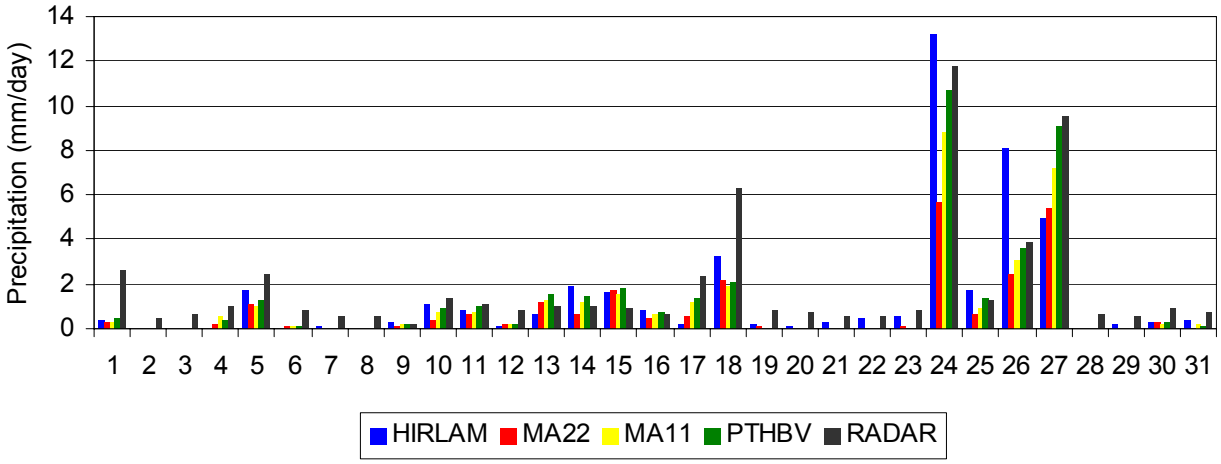

November

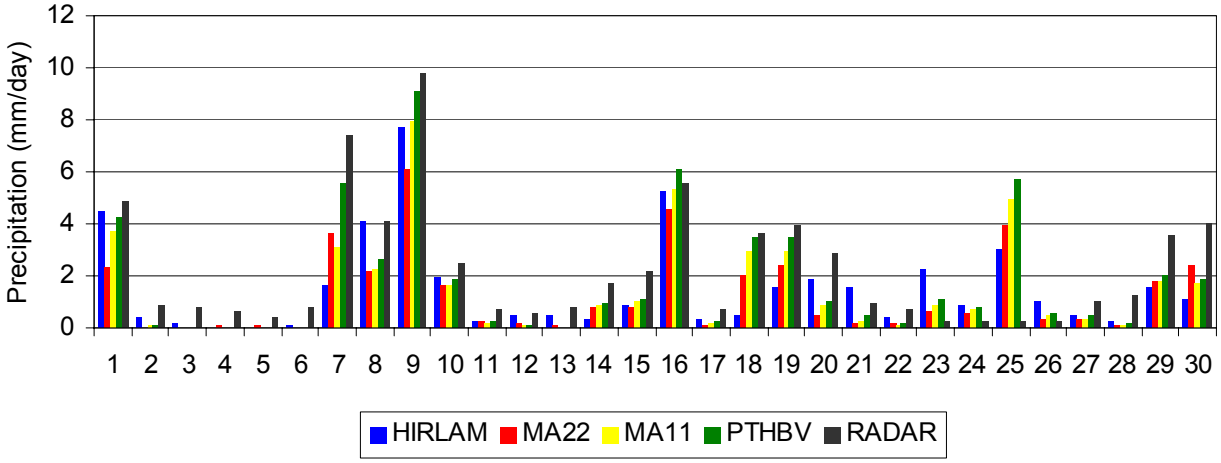

December

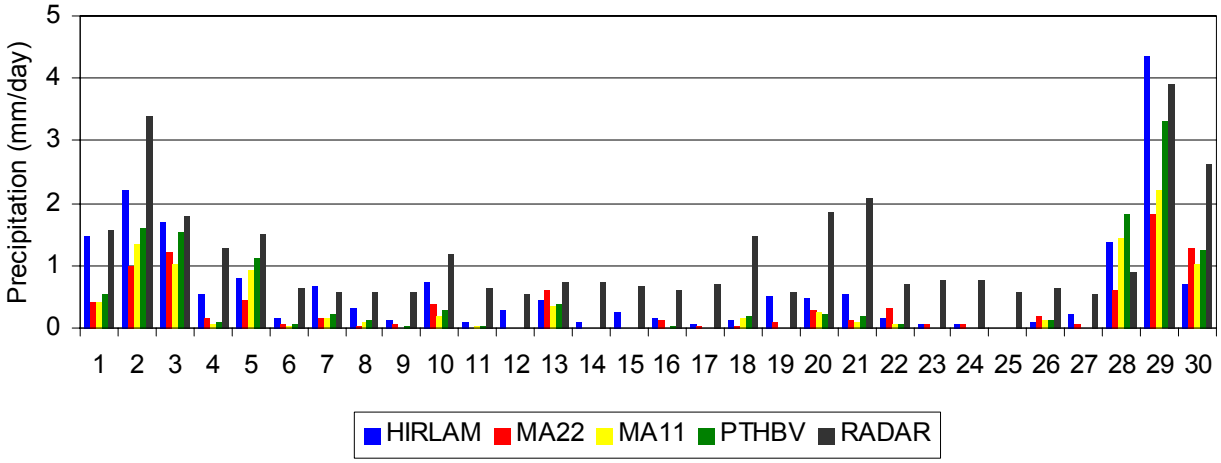

APPENDIX 2 1(2)

Areal distribution of annual total (top to bottom: PTHBV, HIRLAM, RADAR)

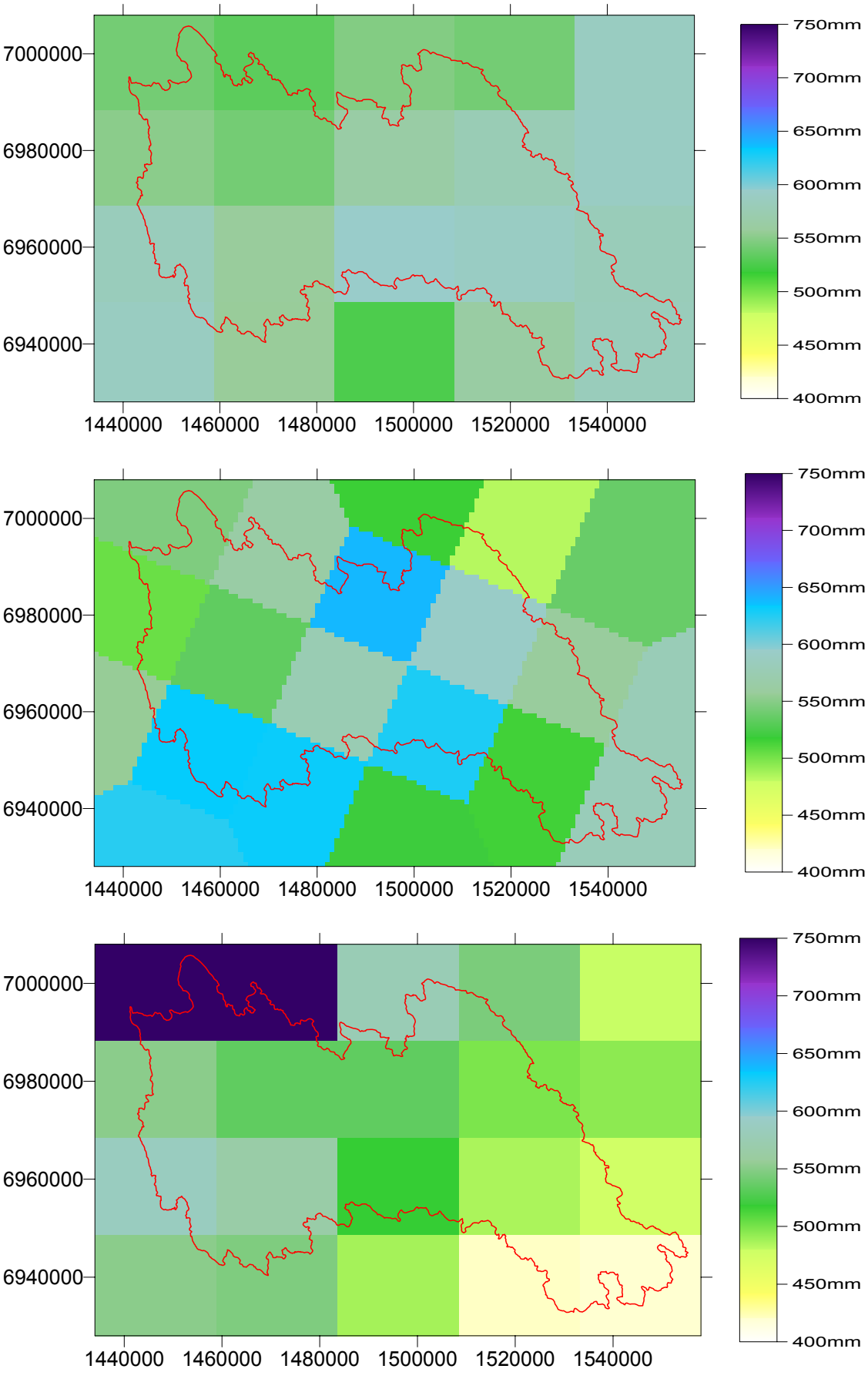

APPENDIX 2 2(2)

Areal distribution of annual total (top to bottom: MA22, MA11)

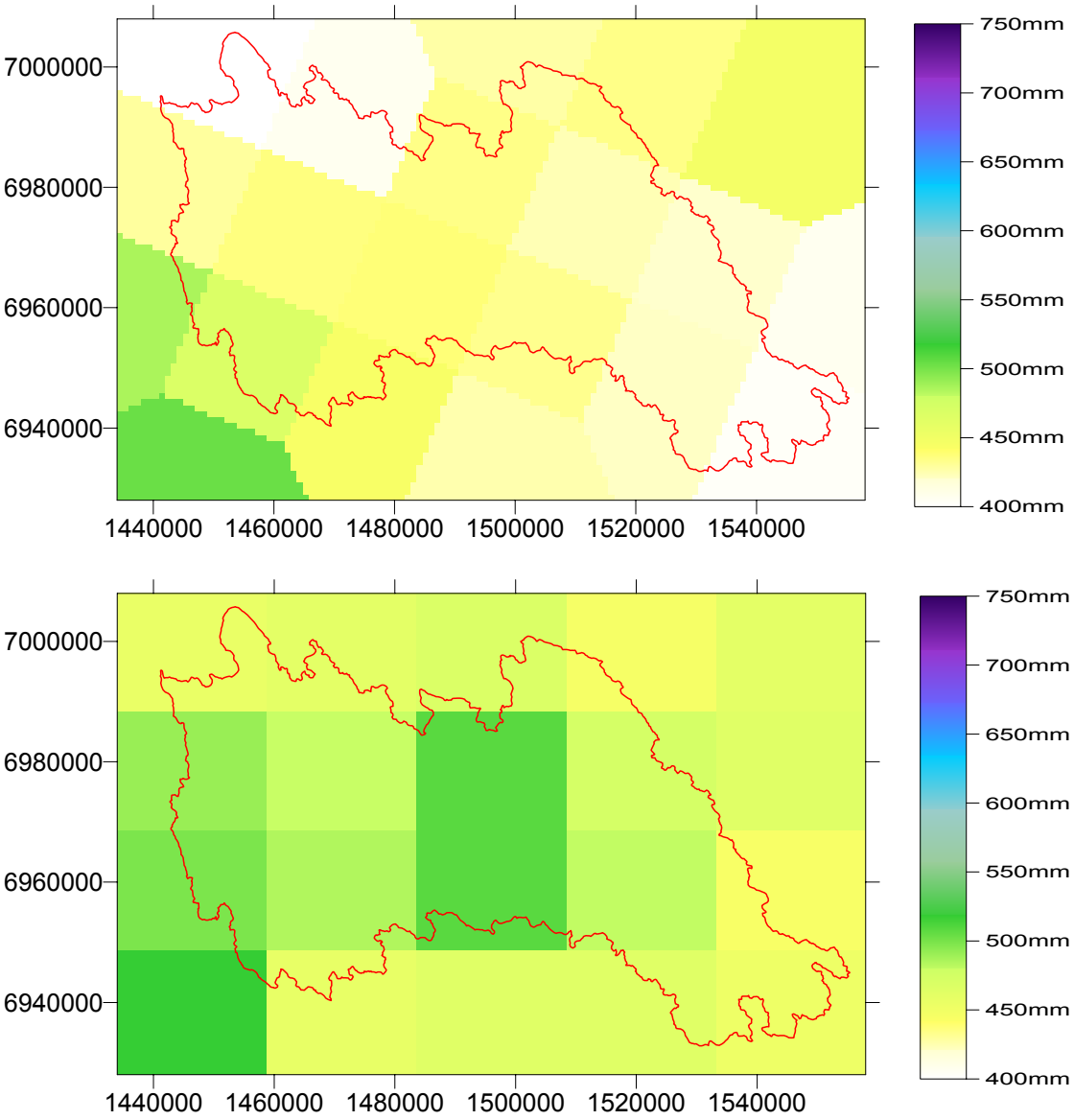

APPENDIX 3 1(2)

Result of HBV-simulation at station Gimdalsbyn (top to bottom: PTHBV, HIRLAM, RADAR).

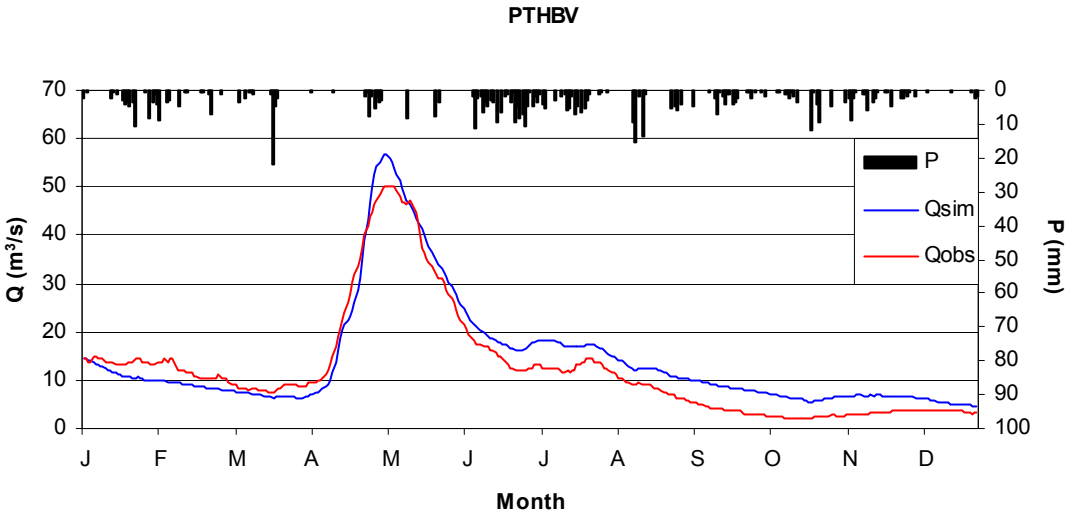

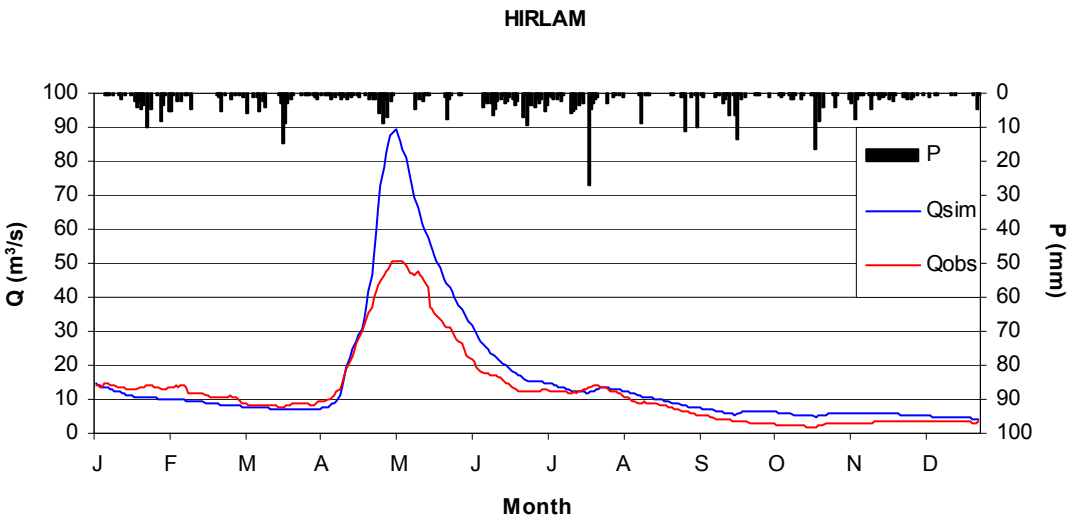

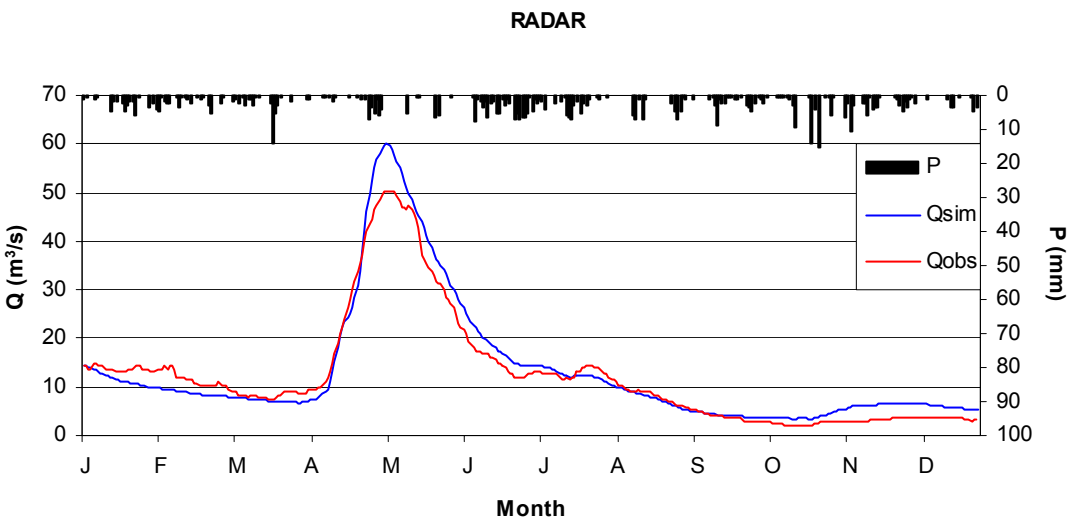

APPENDIX 3 2(2)

Result of HBV-simulation at station Gimdalsbyn (top to bottom: MA22, MA11).

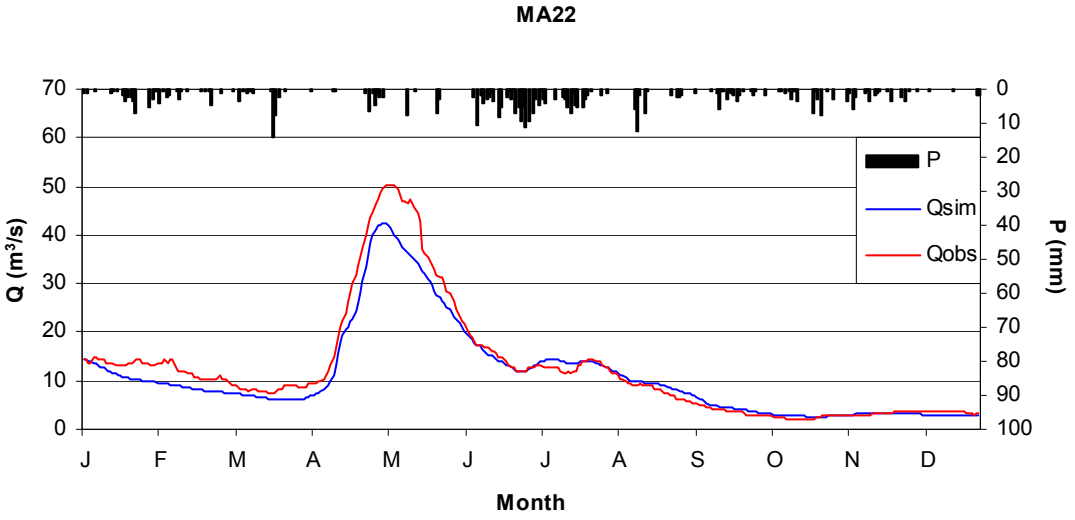

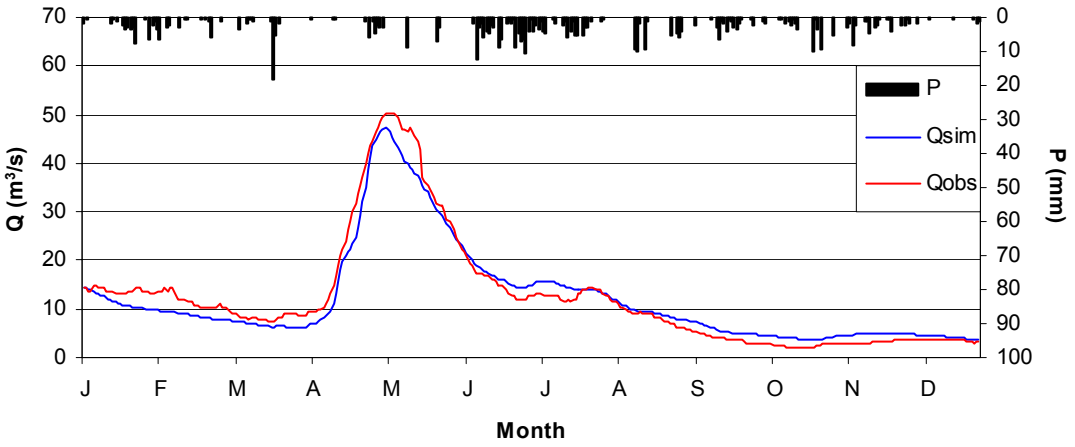

APPENDIX 4 1(2)

Result of HBV-simulation at station Torpshammar (top to bottom: PTHBV, HIRLAM, RADAR).

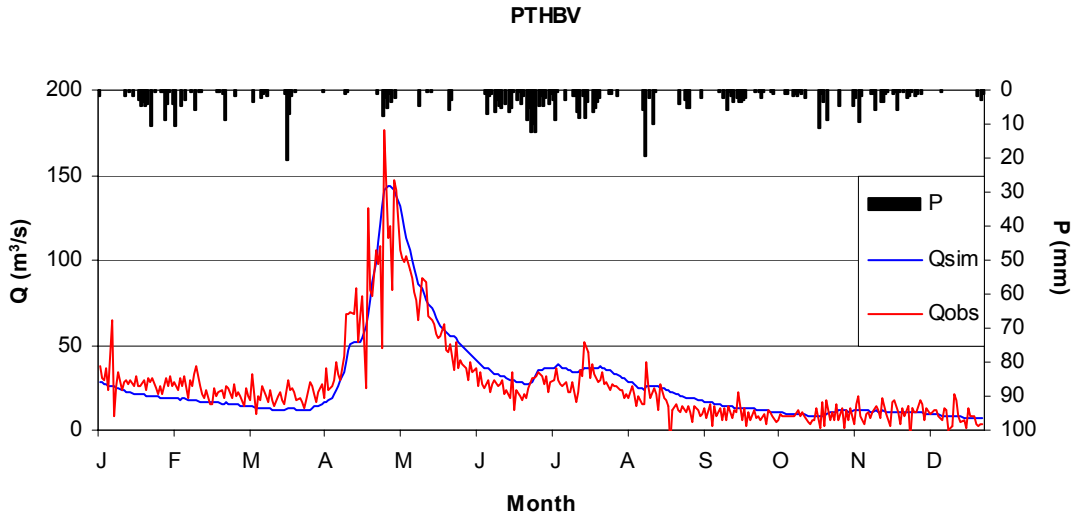

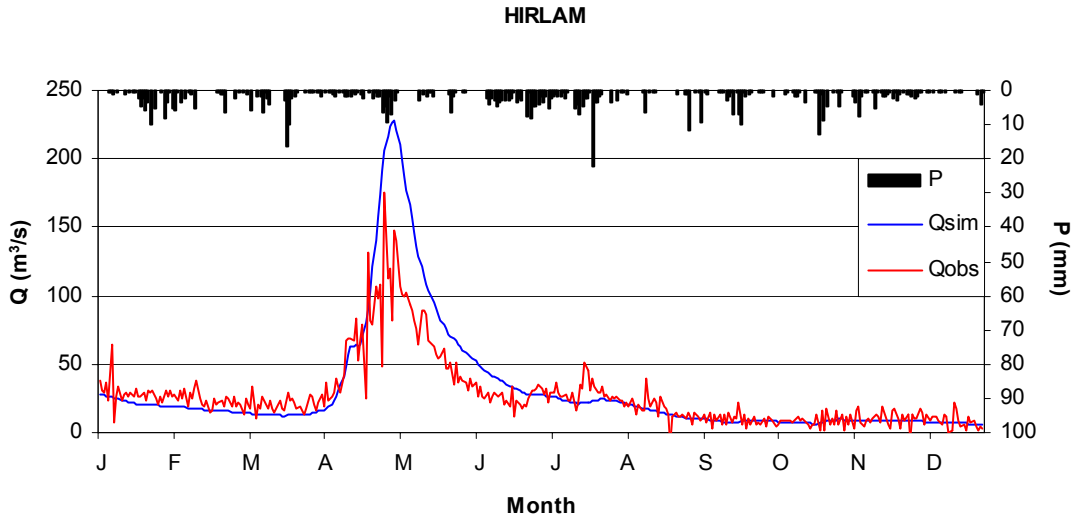

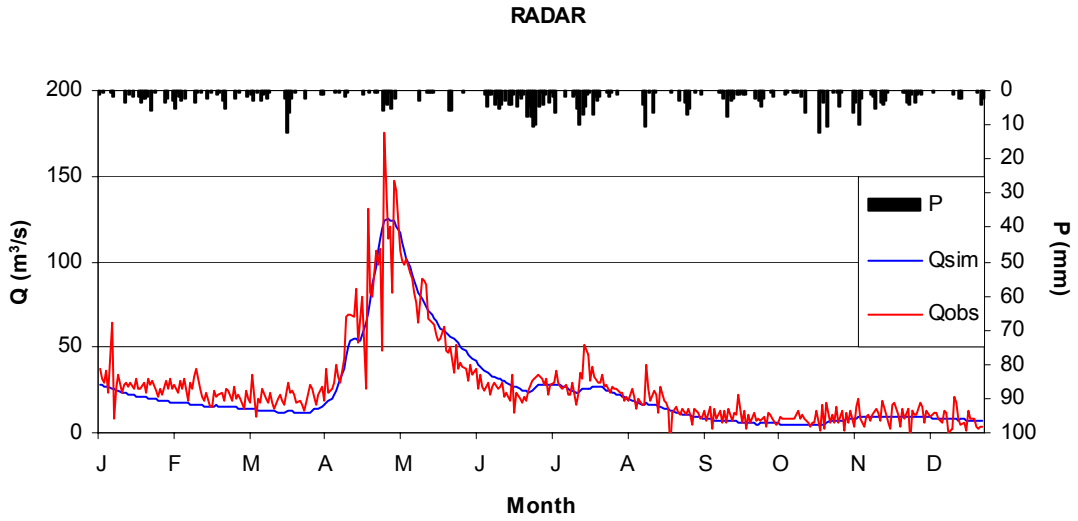

APPENDIX 4 2(2)

Result of HBV-simulation at station Torpshammar (top to bottom: MA22, MA11).

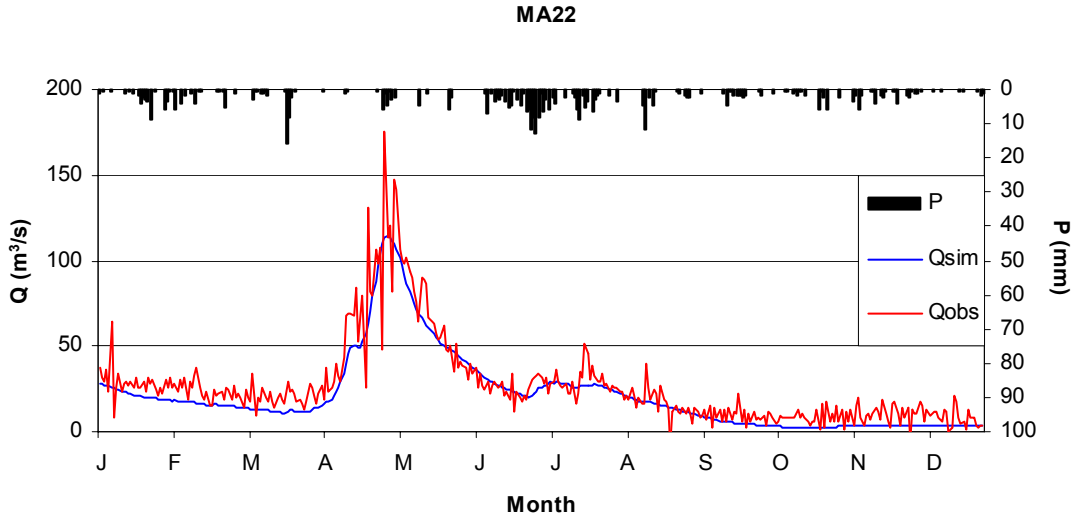

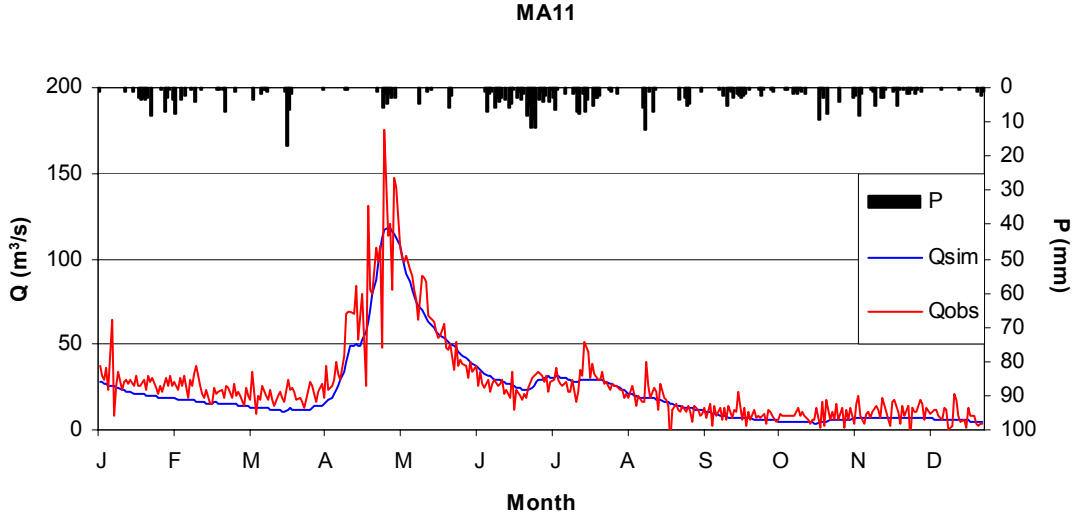

APPENDIX 5 1(4)

Result of HBV forecasting experiment at station Gimdalsbyn 020422-020425.

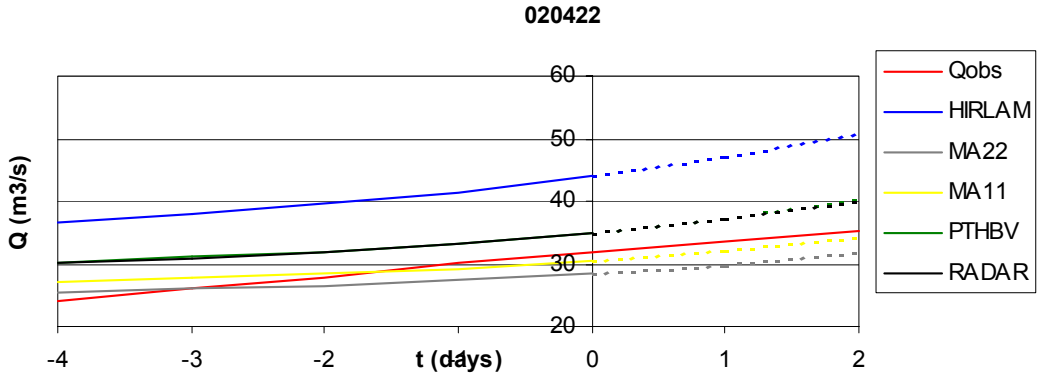

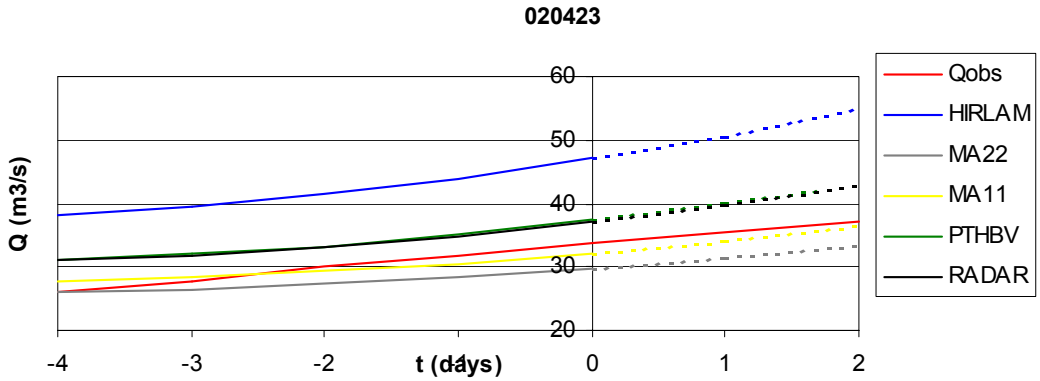

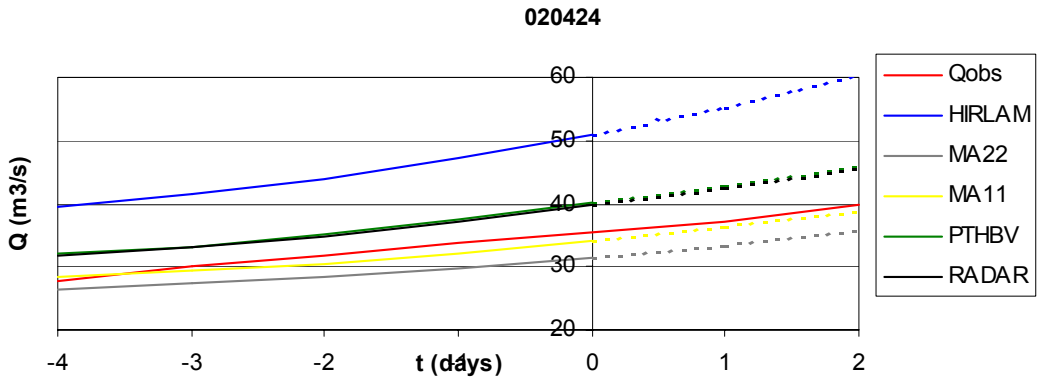

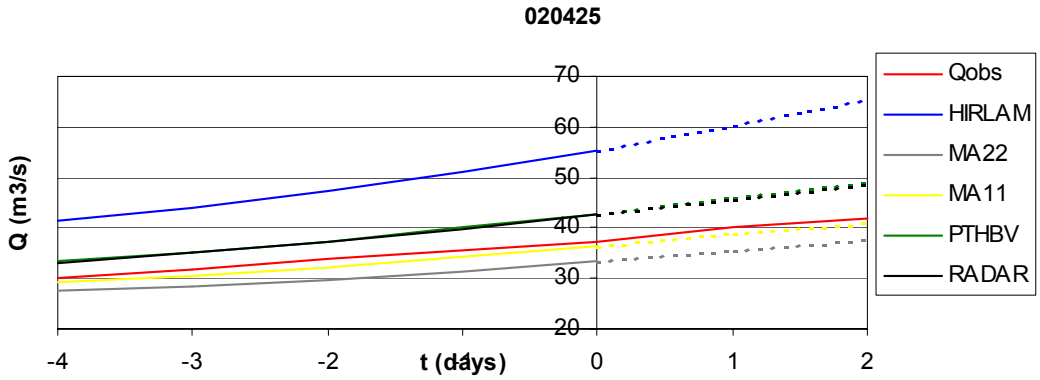

APPENDIX 5 2(4)

Result of HBV forecasting experiment at station Gimdalsbyn 020426-020429.

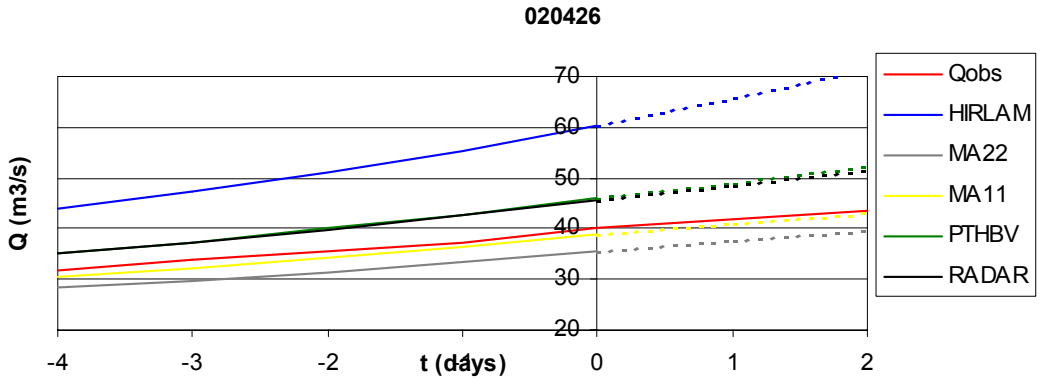

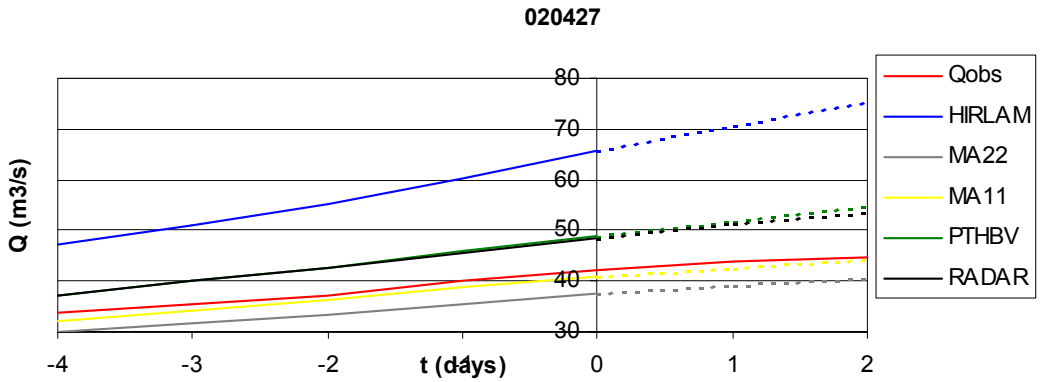

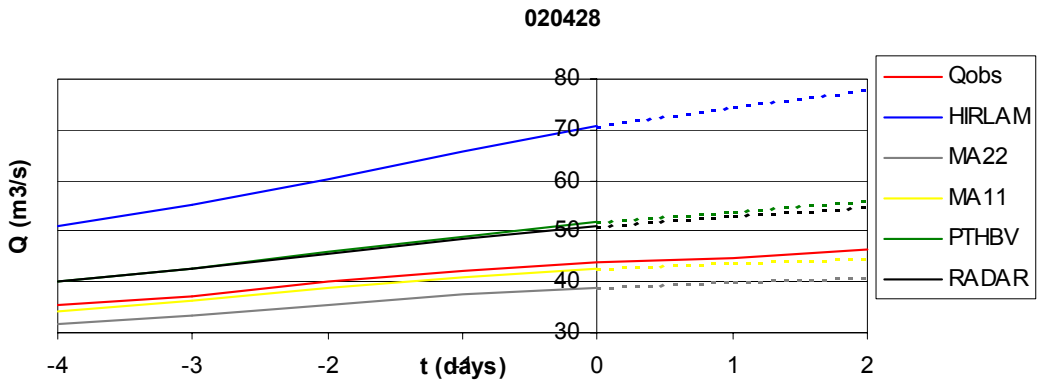

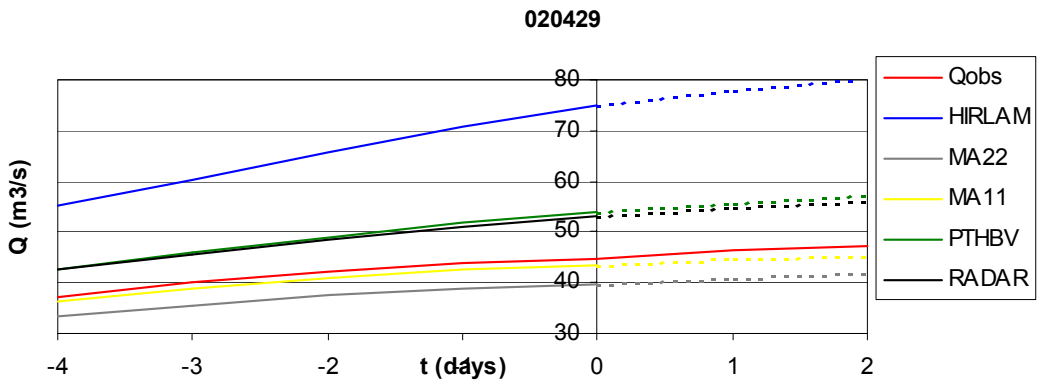

APPENDIX 5 3(4)

Result of HBV forecasting experiment at station Gimdalsbyn 020430-020503.

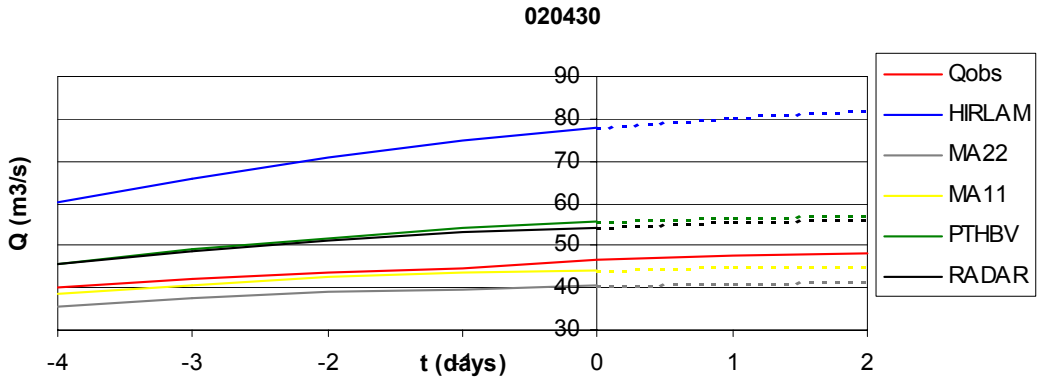

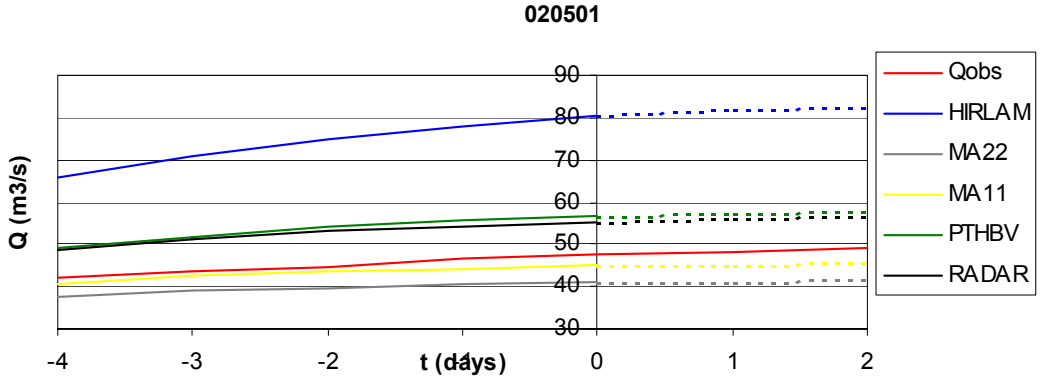

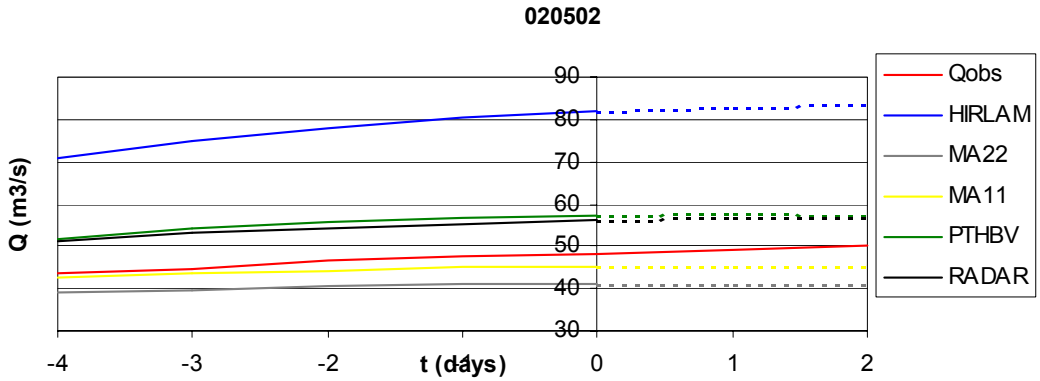

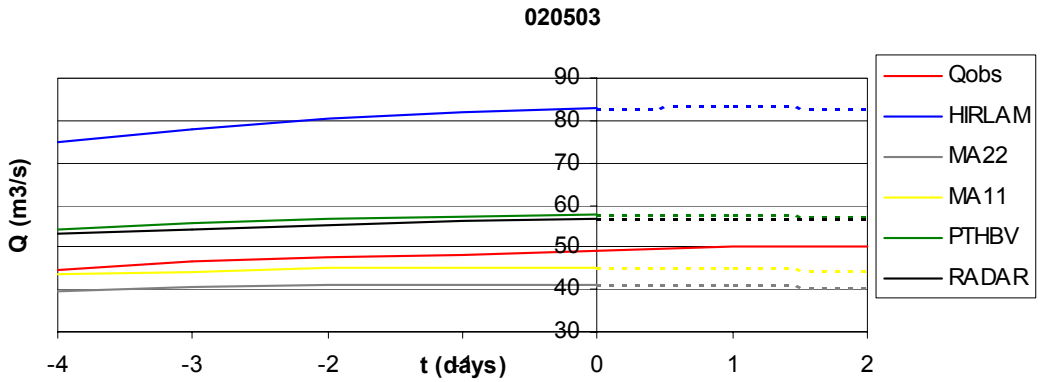

APPENDIX 5 4(4)

Result of HBV forecasting experiment at station Gimdalsbyn 020504-020505.

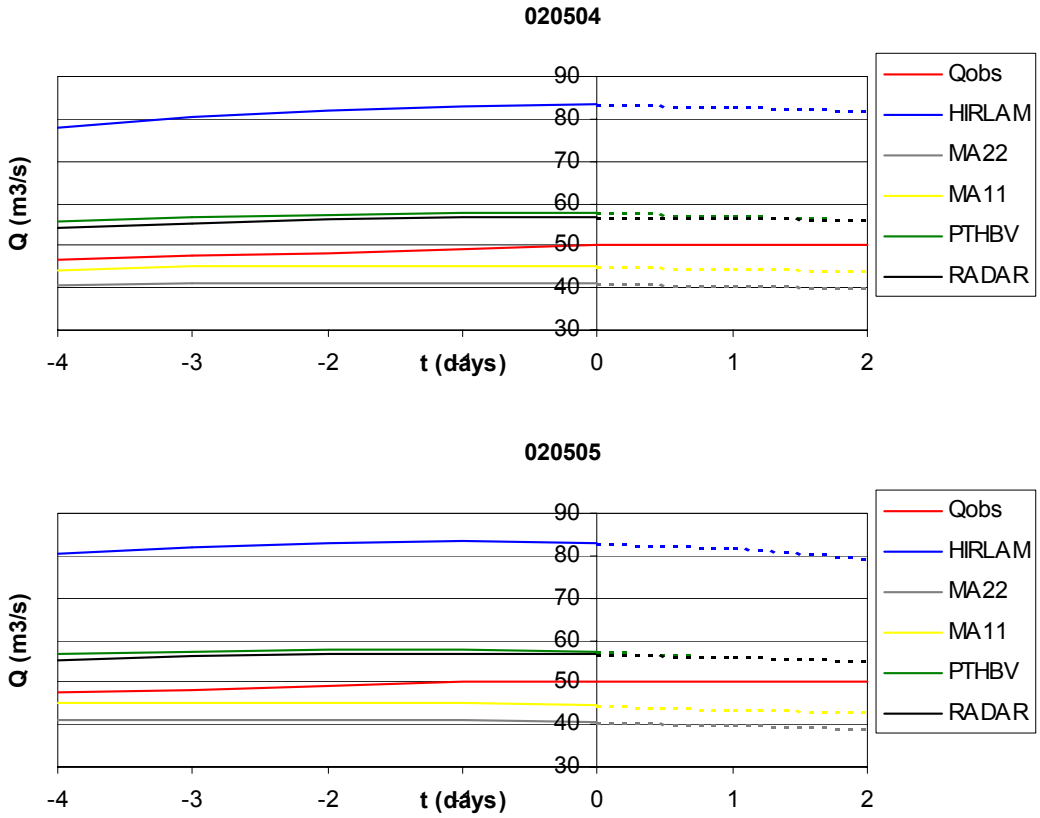

APPENDIX 6 1(4)

Result of HBV forecasting experiment at station Torpshammar 020422-020425.

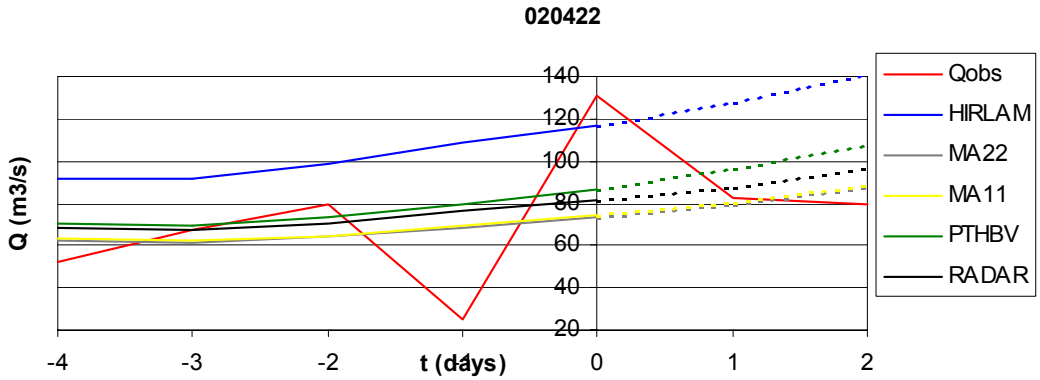

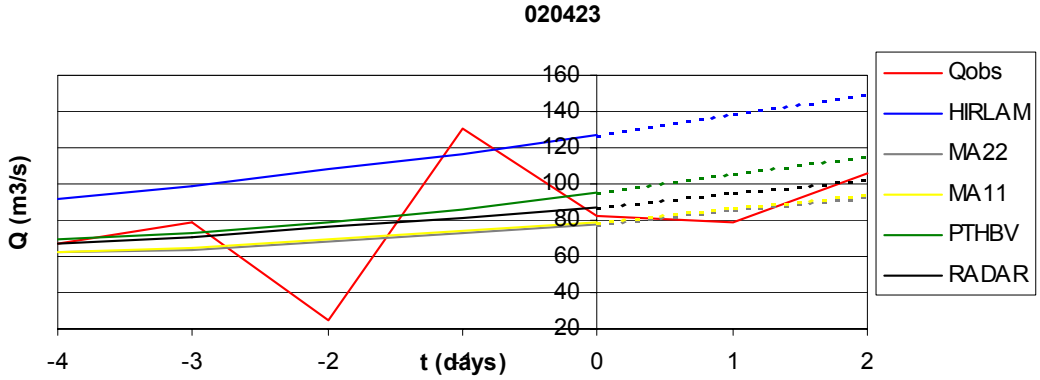

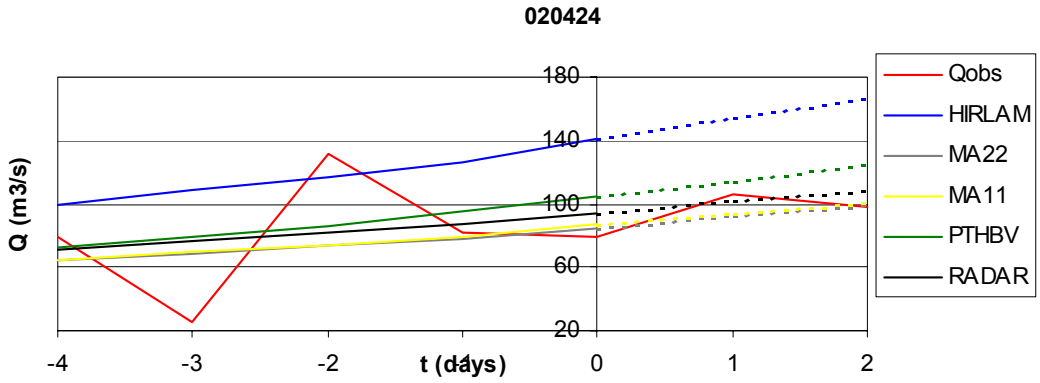

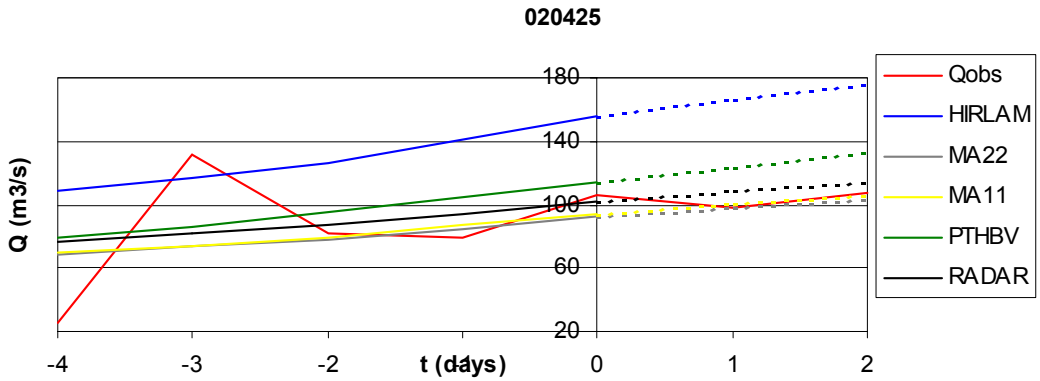

APPENDIX 6 2(4)

Result of HBV forecasting experiment at station Torpshammar 020426-020429.

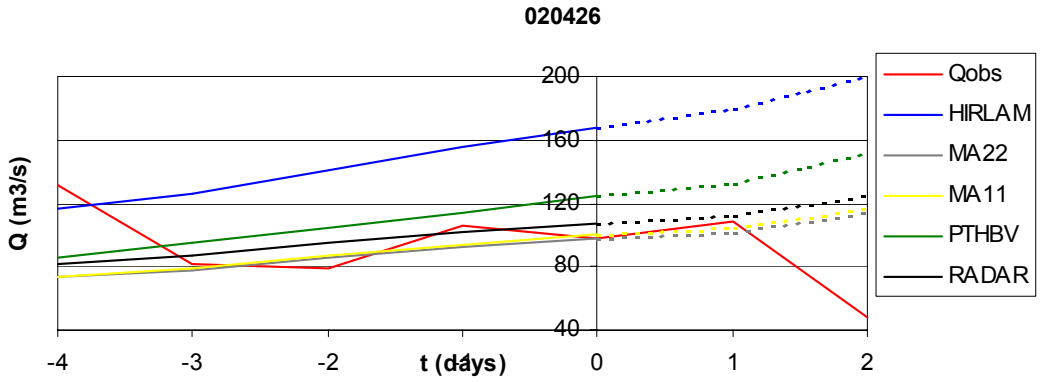

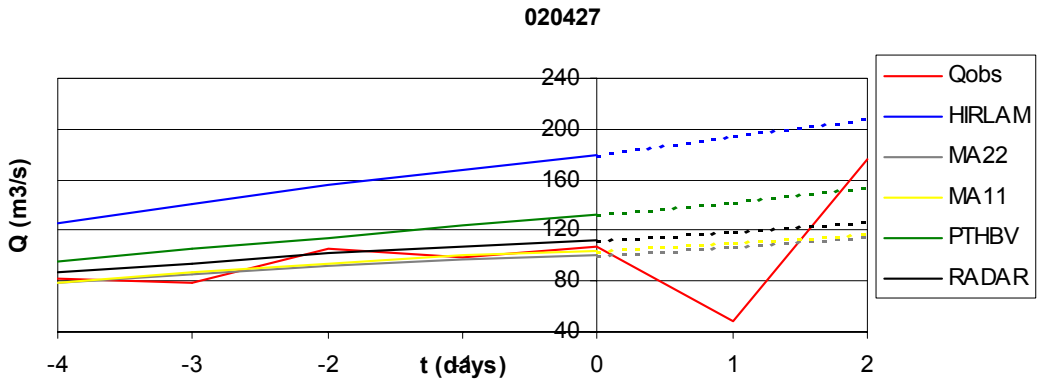

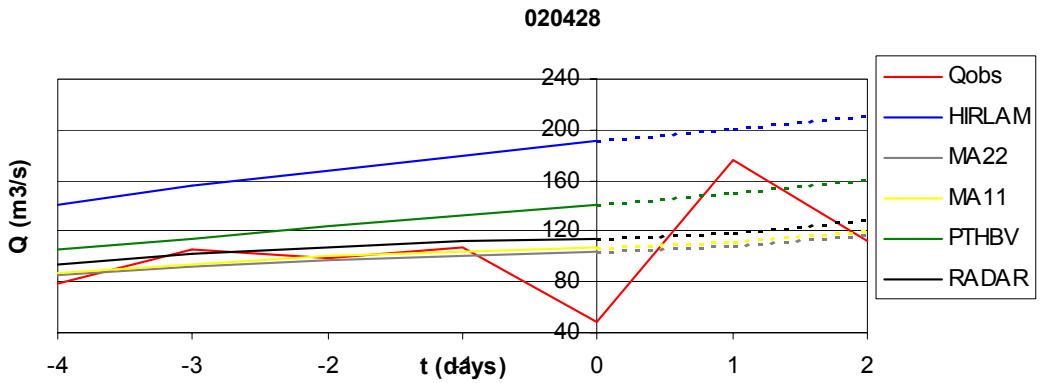

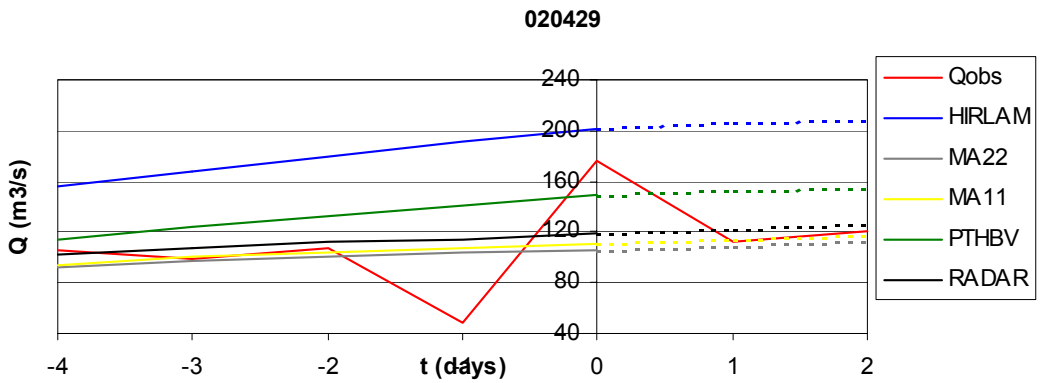

APPENDIX 6 3(4)

Result of HBV forecasting experiment at station Torpshammar 020430-020503.

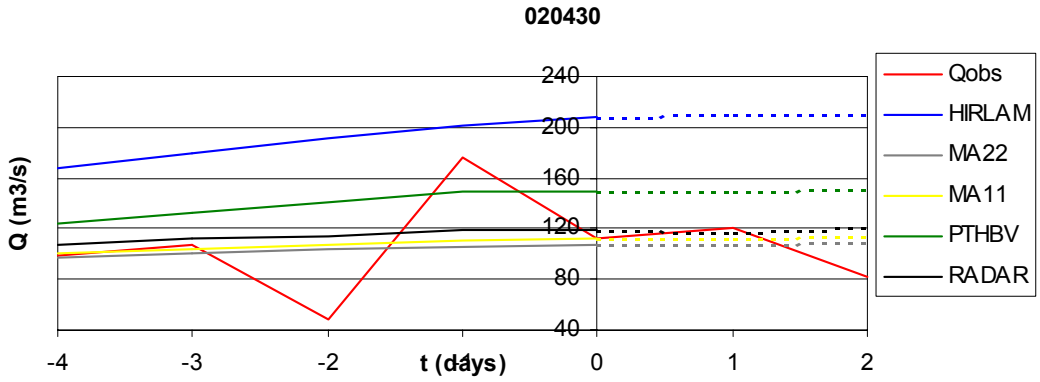

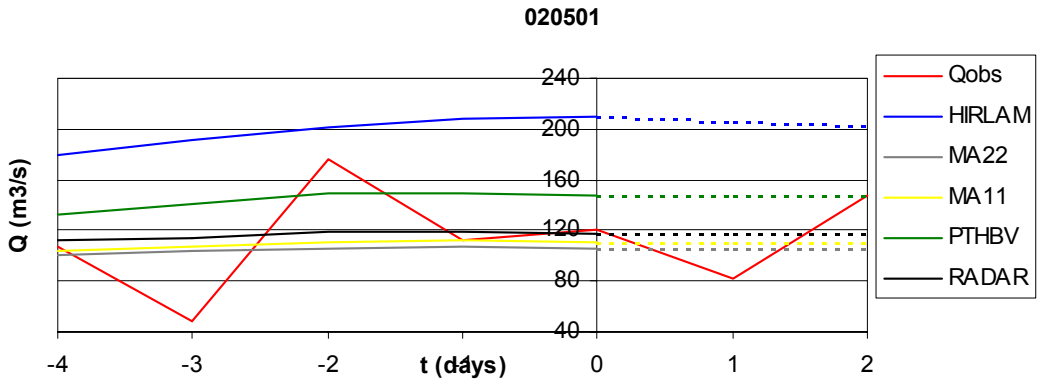

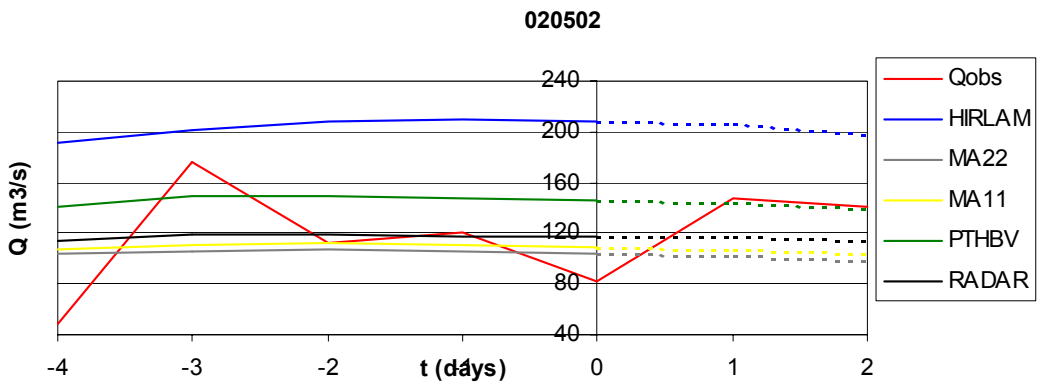

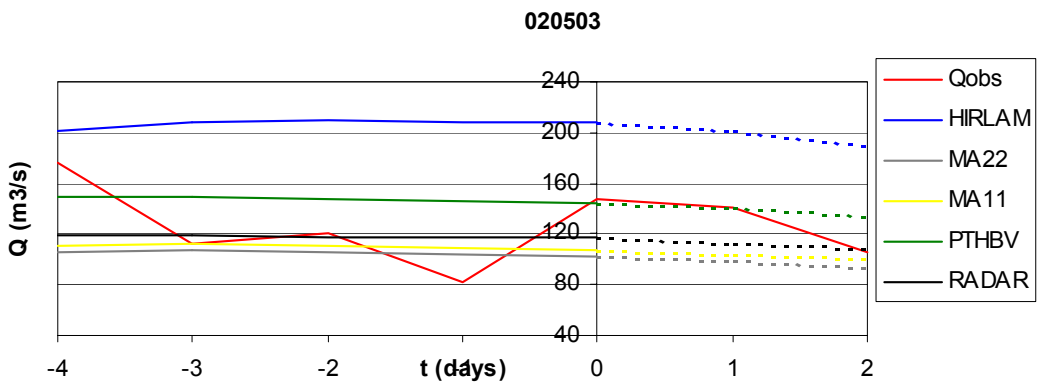

APPENDIX 6 4(4)

Result of HBV forecasting experiment at station Torpshammar 020504-020505.